Epitaxy studies with Low Energy Electron Microscopy (LEEM)

E. Bauer
Arizona State University, Tempe, Arizona, USA

Outline

Pre-LEEM work
Some Basics of LEEM
Quasi-monolayer-by-monolayer growth
Interfactant-mediated growth
Transition from two- to three-dimensional growth
Reactive growth
Three-dimensional growth
Some basics of SPELEEM + application
Stress anisotropy
Summary

Pre-LEEM work

Until 1934: Light microscopy (crystallography, mineralogy, chemistry)

From 1934: Electron diffraction (physics)

From 1956: Transmission electron microscopy (physics) [1,2]

1958: Growth classification [3]

- Frank-van der Merwe (layer-by-layer) growth (FM)
- Stranski-Krastanov (layer-plus-island) growth (SK)
- Volmer-Weber (island) growth (VW)

Determined by:

- Substrate surface energy γ_s
- Film surface energy γ_f
- Interface energy γ_i (strain energy)

Requirements for well-defined growth studies:

ultrahigh vacuum

Surface-sensitive, nondestructive imaging method

Around 1960 birth of surface science: metal UHV systems

LEED, but no lateral resolution!

[1] E. Bauer, Z. Kristallogr. 107 (1956) 265
[2] E. Bauer, Z. Kristallogr. 110 (1958) 395
[3] E. Bauer, Z. Kristallogr. 110 (1958) 372

Origin of LEEM

JOURNAL OF APPLIED PHYSICS VOLUME 31, NUMBER 12 DECEMBER, 1960

Oxygen on Nickel

L. H. GERMER AND C. D. HARTMAN
Bell Telephone Laboratories, Murray Hill, New Jersey
(Received August 4, 1960)

LEED study

PHYSICAL REVIEW VOLUME 123, NUMBER 4 AUGUST 15, 1961

Interpretation of Low-Energy Electron Diffraction Patterns of Adsorbed Gases

ERNST BAUER
Michelson Laboratory, China Lake, California
(Received March 27, 1961)

Germer

single scattering

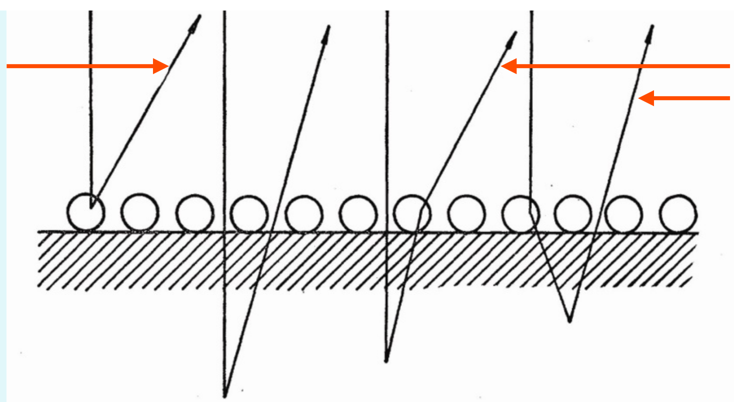

Bauer

double scattering

To eliminate such ambiguities, **low-energy electron diffraction** investigations ….on single-crystal surfaces **should be combined with** other techniques, e.g., **electron microscopy**…..

A program along these lines is in progress in this laboratory

LEEM schematic

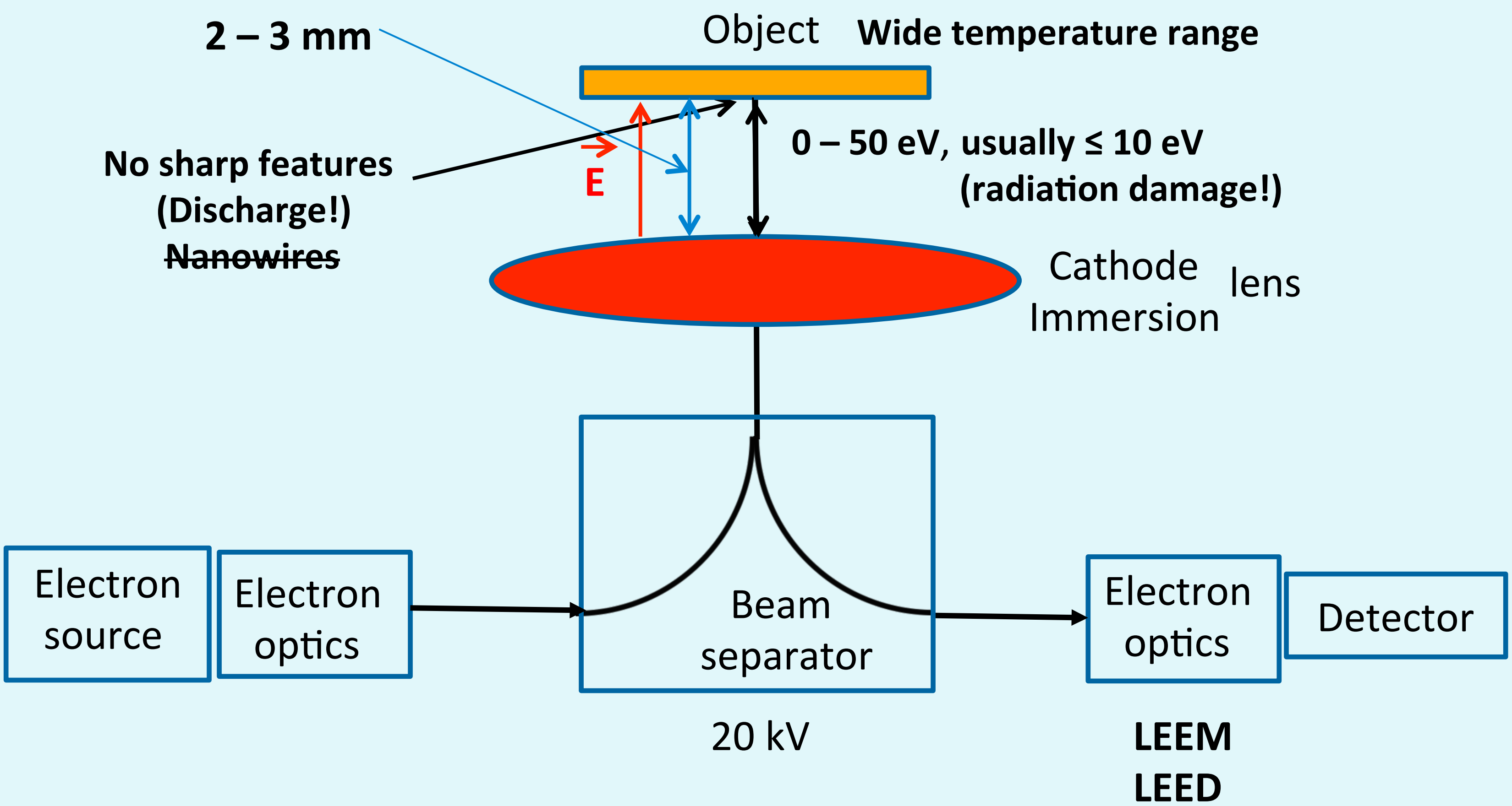

Illuminated region typically ≤ 100 µm diameter

In-situ evaporation and gas exposure at grazing angle of incidence 16° - 45°

Pressure ≤ 10^{-5} mbar

LEEM 1985

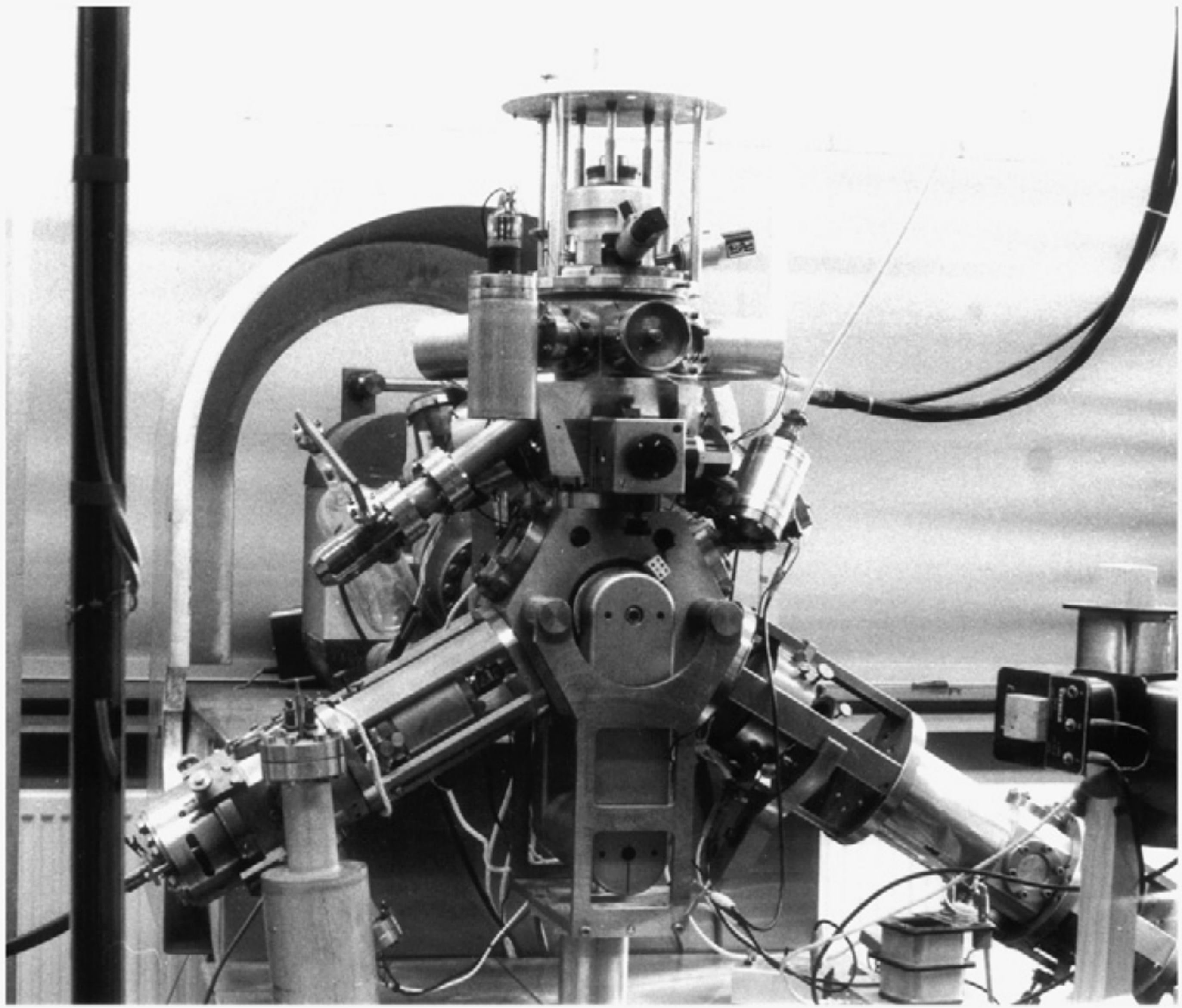

LEEM 2015

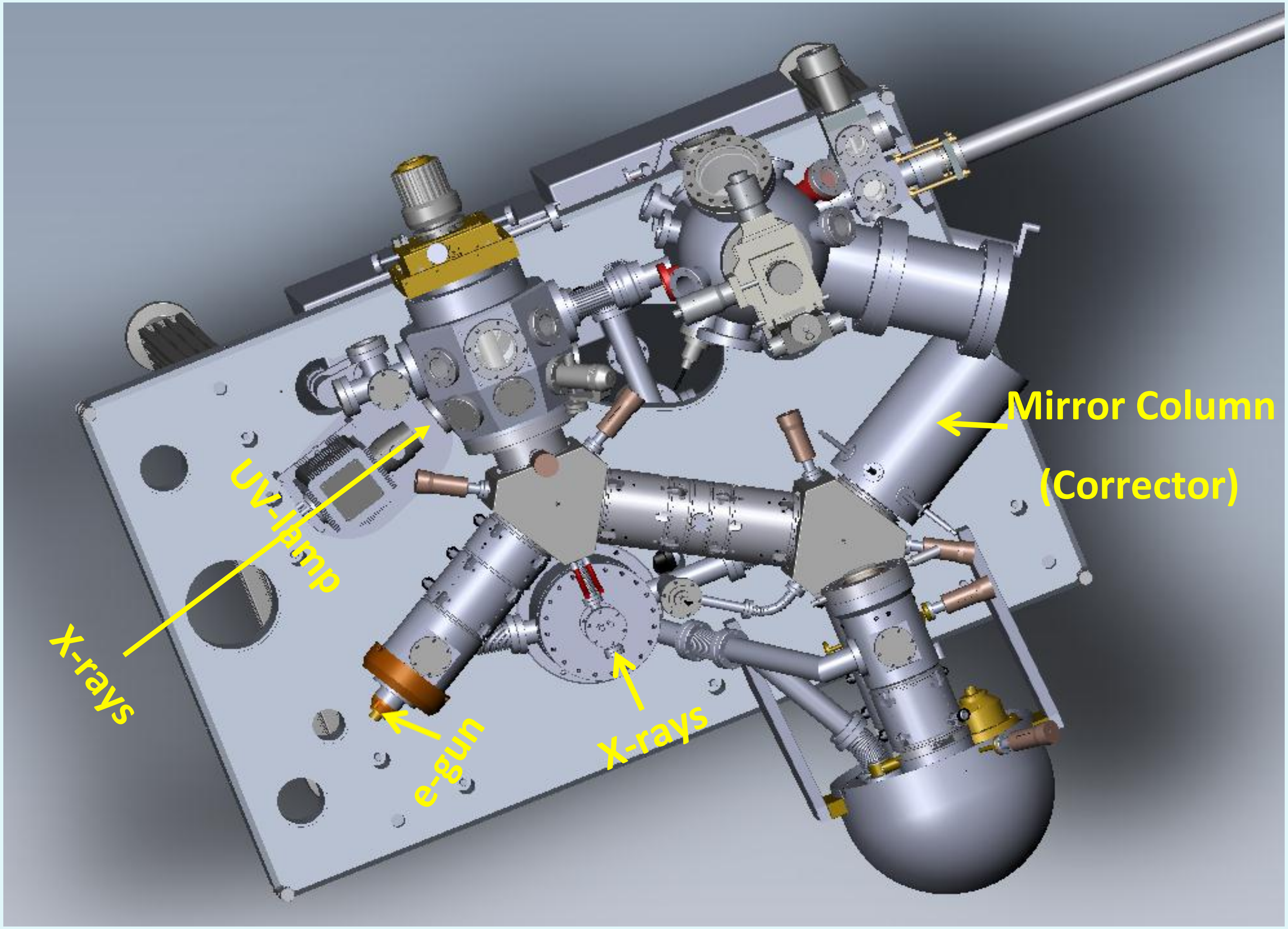

Aberration-corrected spectroscopic photoemission and low energy electron microscope (SPELEEM}

Resolution

Determined by chromatic and spherical aberration of objective lens

Without aberration correction ≈ 5 nm

With aberration correction ≈ 1 nm (not achieved yet)

Intensity

Reflected intensity concentrated in diffraction beams

At low energies intensity of specular beam as high as 70%

Allows image acquisition at video rates

Contrast

Diffraction contrast:

Bright-field ((00) beam): normal periodicity

Dark-field ((hk) beams): lateral periodicity

Phase contrast: steps

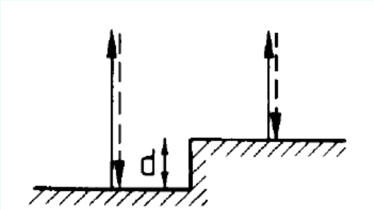

Quantum size contrast: thickness

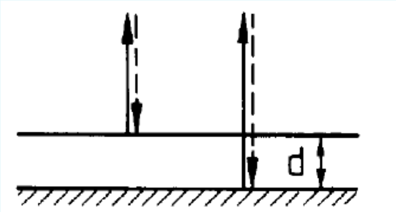

Diffraction contrast (first good LEEM images 1985)

Si(111) – (1×1)→ (7×7) Coexistence

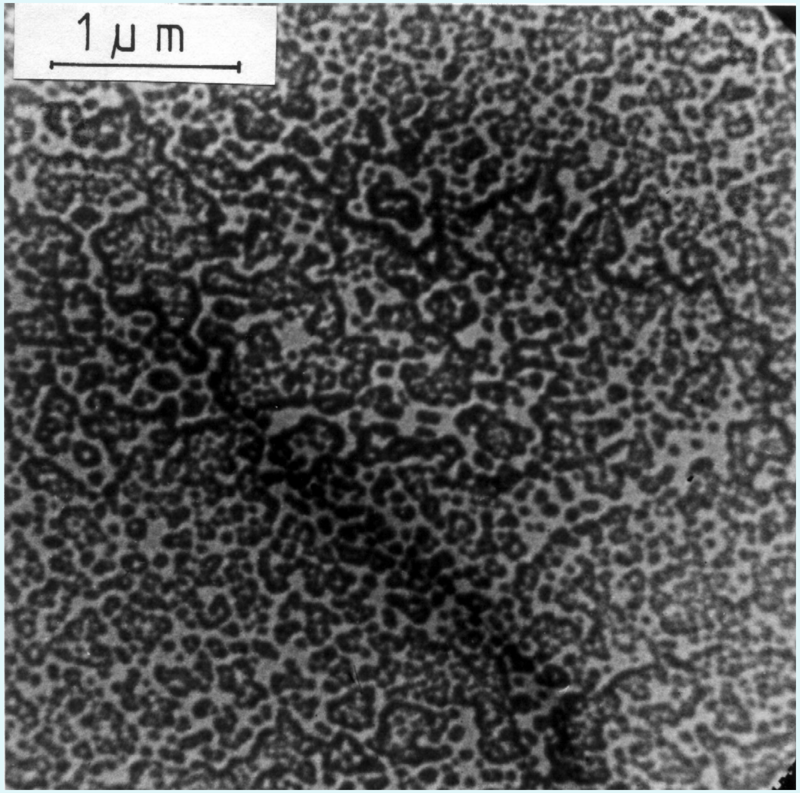

11 eV

After long anneal at 1150 K

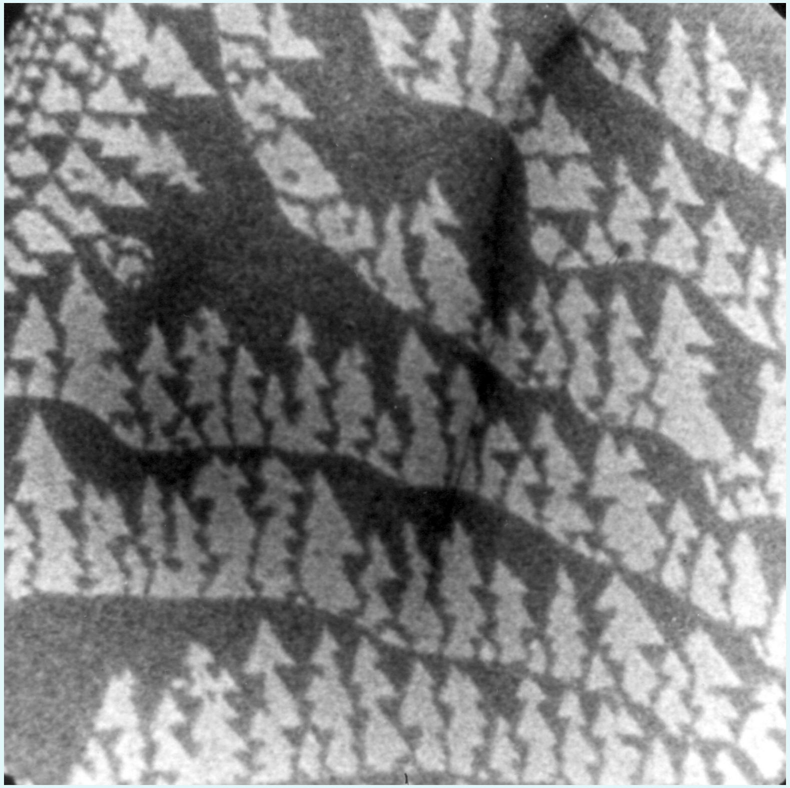

10.5 eV

After quenching from 1450 K

Both surfaces show an excellent (7×7) LEED pattern!

W. Telieps and E. Bauer, Ultramicroscopy 17, 57 (1985)1985

Quasi-monolayer-by-monolayer growth
(Frank-van der Merwe growth)

$$\gamma_f + \gamma_i \leq \gamma_s$$

Homoepitaxy $\gamma_f = \gamma_s, \ \gamma_i = 0$

Large anisotropy of
step free energy:
$E_B > 2.6\ E_A$ at 800 K
Surface stress anisotropy

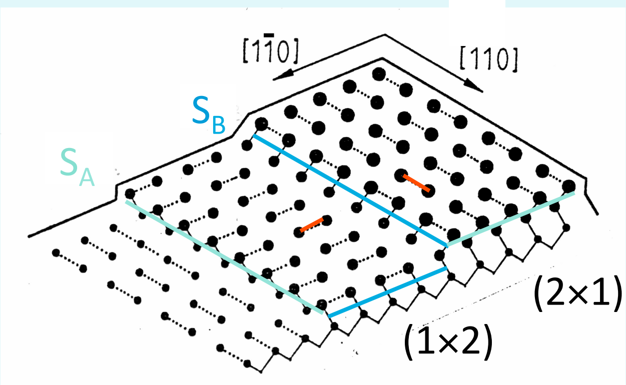

Terraces alternate in dimer direction

Low supersaturation:
Nucleation of new layer at
reantrant corner (defect)

Anisotropic growth of Si(100)

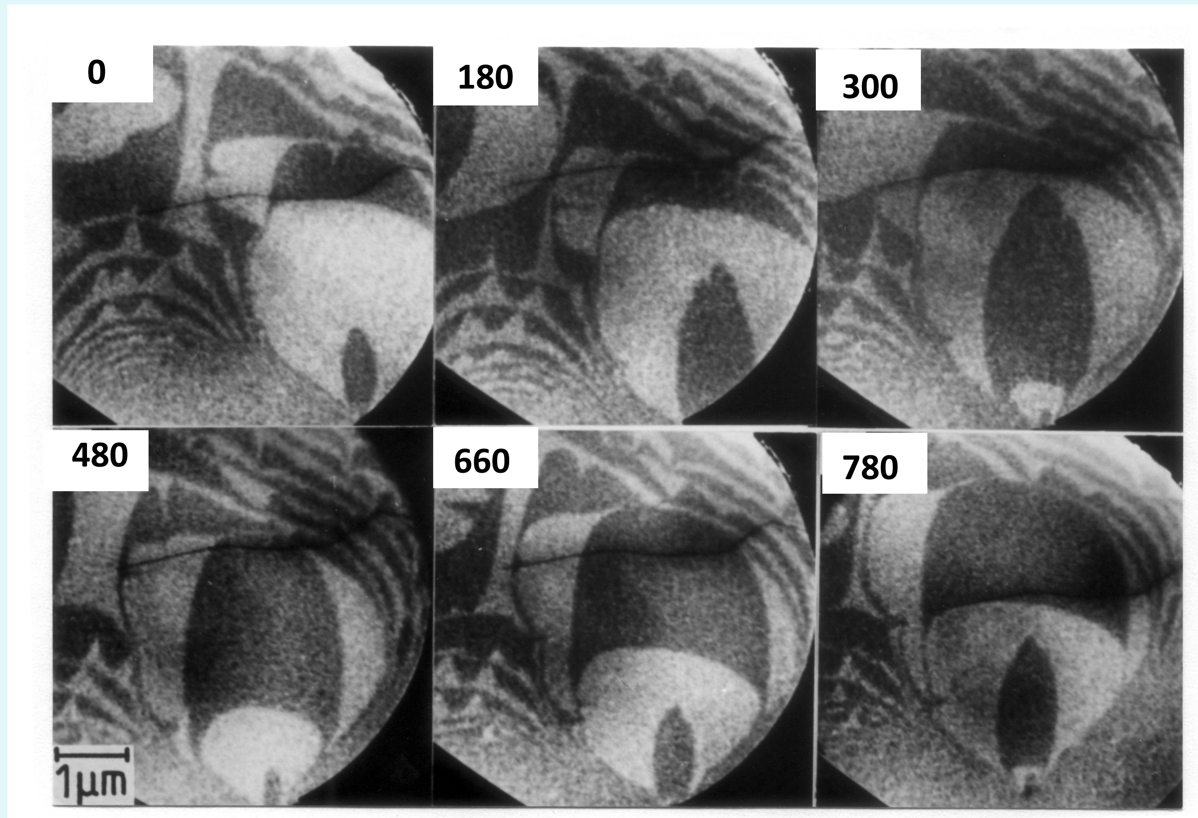

800 K, video frames, E = 5 eV, numbers: sec

W. Święch and E.Bauer, Surf.Sci. 255, 219

Frank-van der Merwe growth

Homoepitaxy

Anisotropic growth of Si(100)

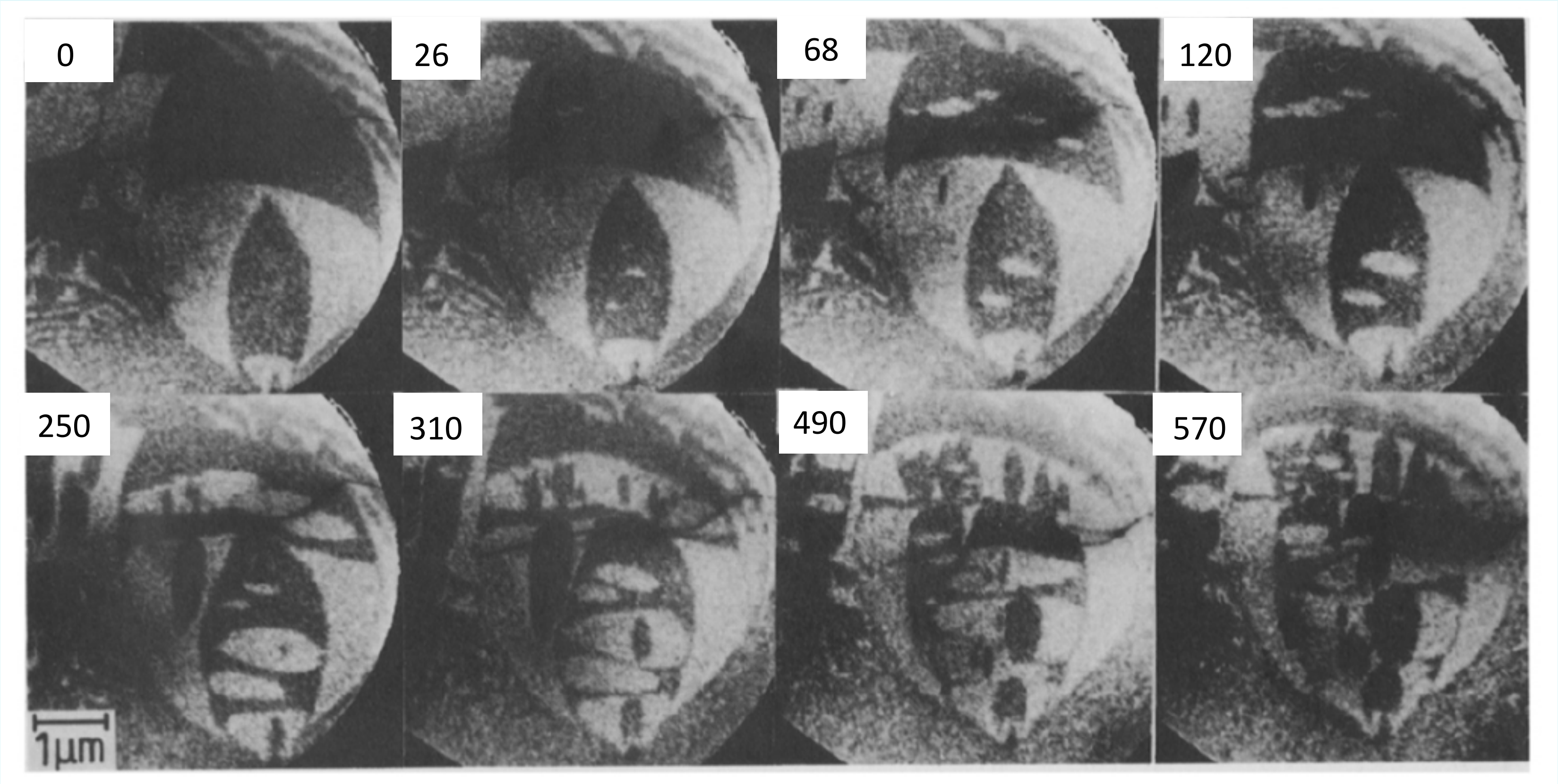

650 K, video frames, E = 5 eV, numbers: sec

Higher supersaturation:
Nucleation of new layer on
Terraces: multi-level growth

For more information see:
W. Theis and R. M. Tromp, Phys. Rev. Lett. 76, 2770 (1996)
V. Zielasek et al, Phys. Rev. B 64, 201320 (2001)

W. Święch and E.Bauer, Surf.Sci. 255, 219 (1991)

Frank-van der Merwe growth

Homoepitaxy

Spiral growth + island nucleation on terraces. Example: Pb(111)

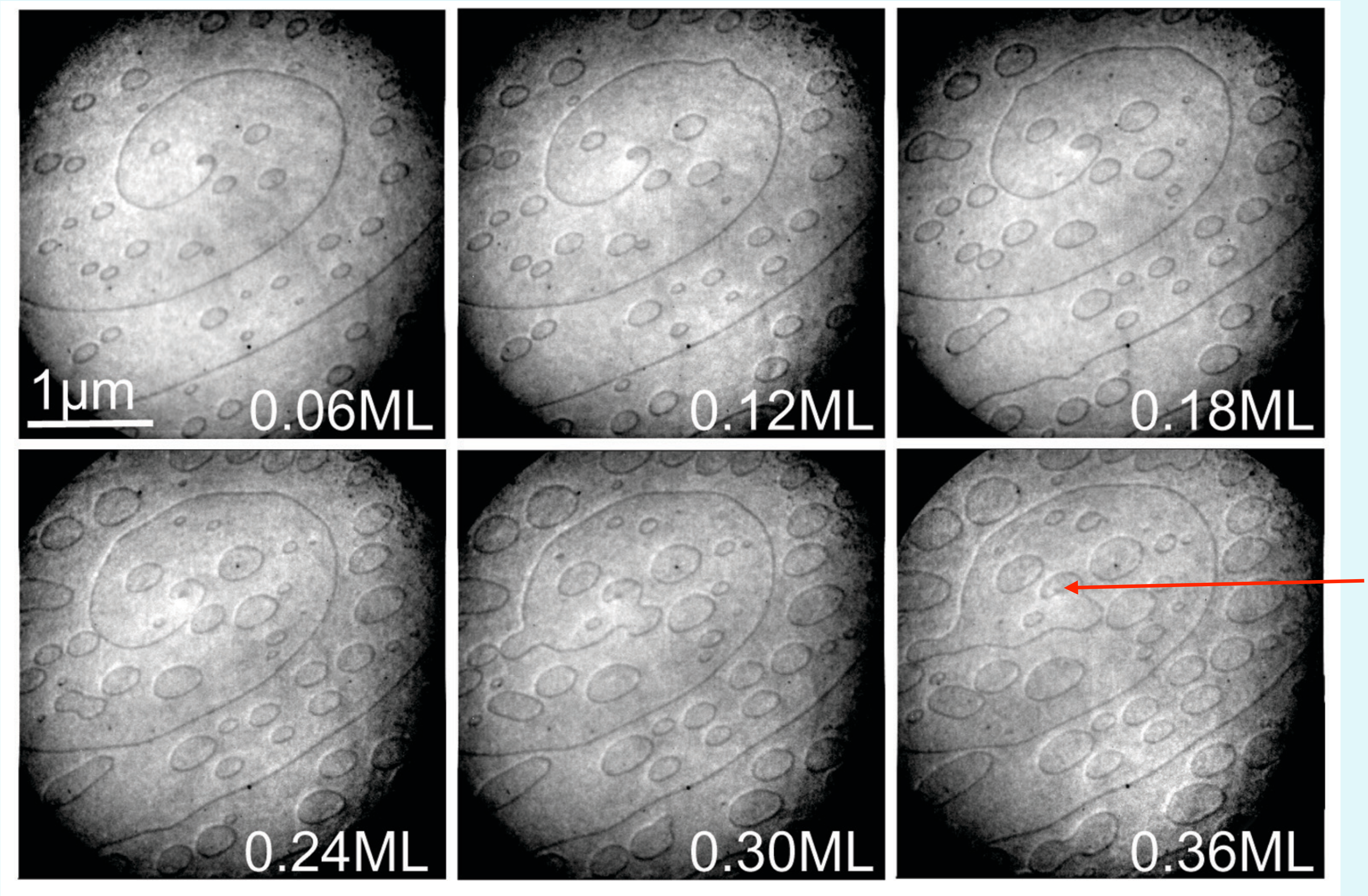

Video frames, 8.6 eV, room temperature

Th. Schmidt and E. Bauer, at Elettra, 1998

Frank-van der Merwe growth

Heteroepitaxy $\gamma_f < \gamma_s$ $\gamma_i > 0$ (strain!)

Strain relaxation by interfactant

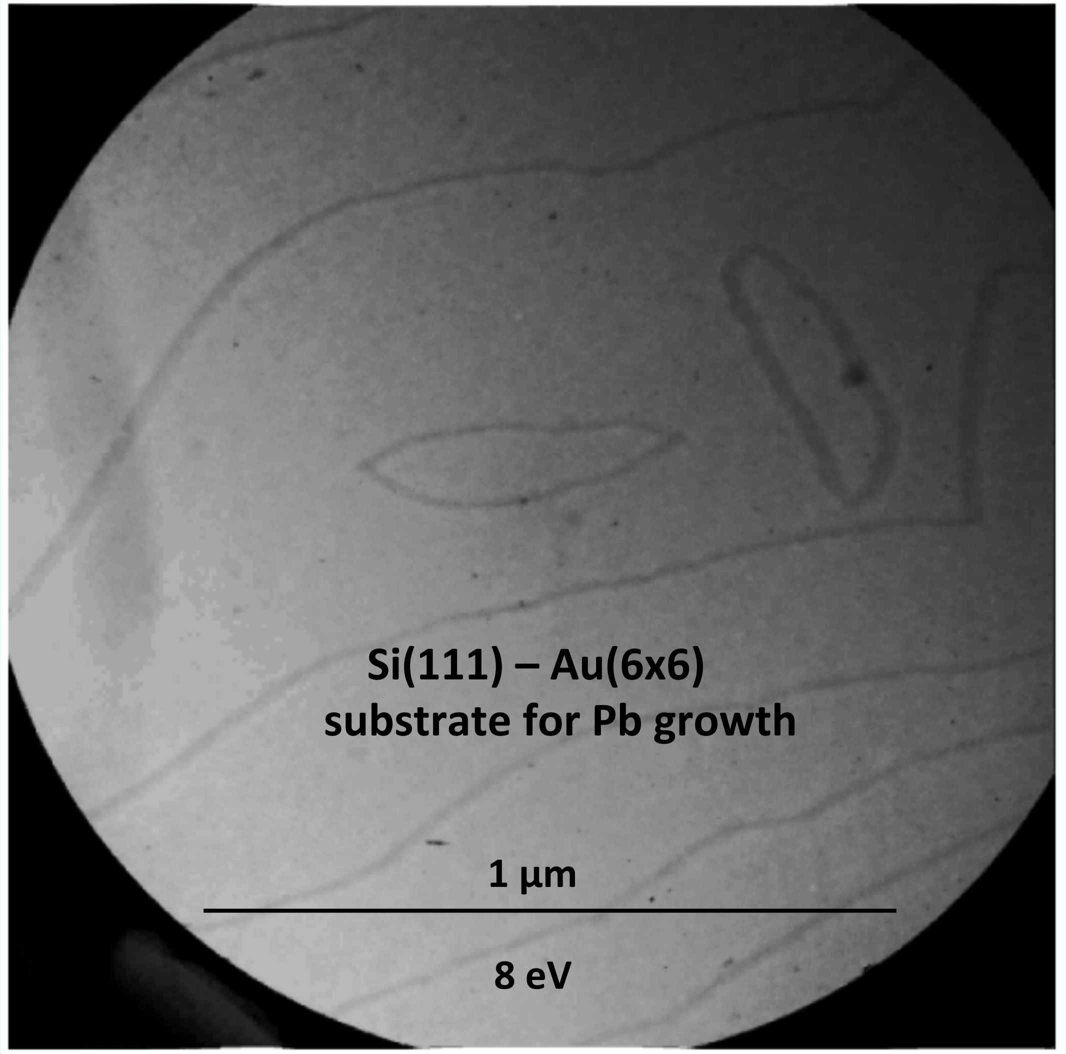

Th. Schmidt and E. Bauer, Phys. Rev. B 62 (2000) 15815; Ag interfactant: Surf. Sci. 480 (2001) 137

Frank-van der Merwe growth

Interfactant-mediated: Pb / Si(111)- Au(6x6) Au

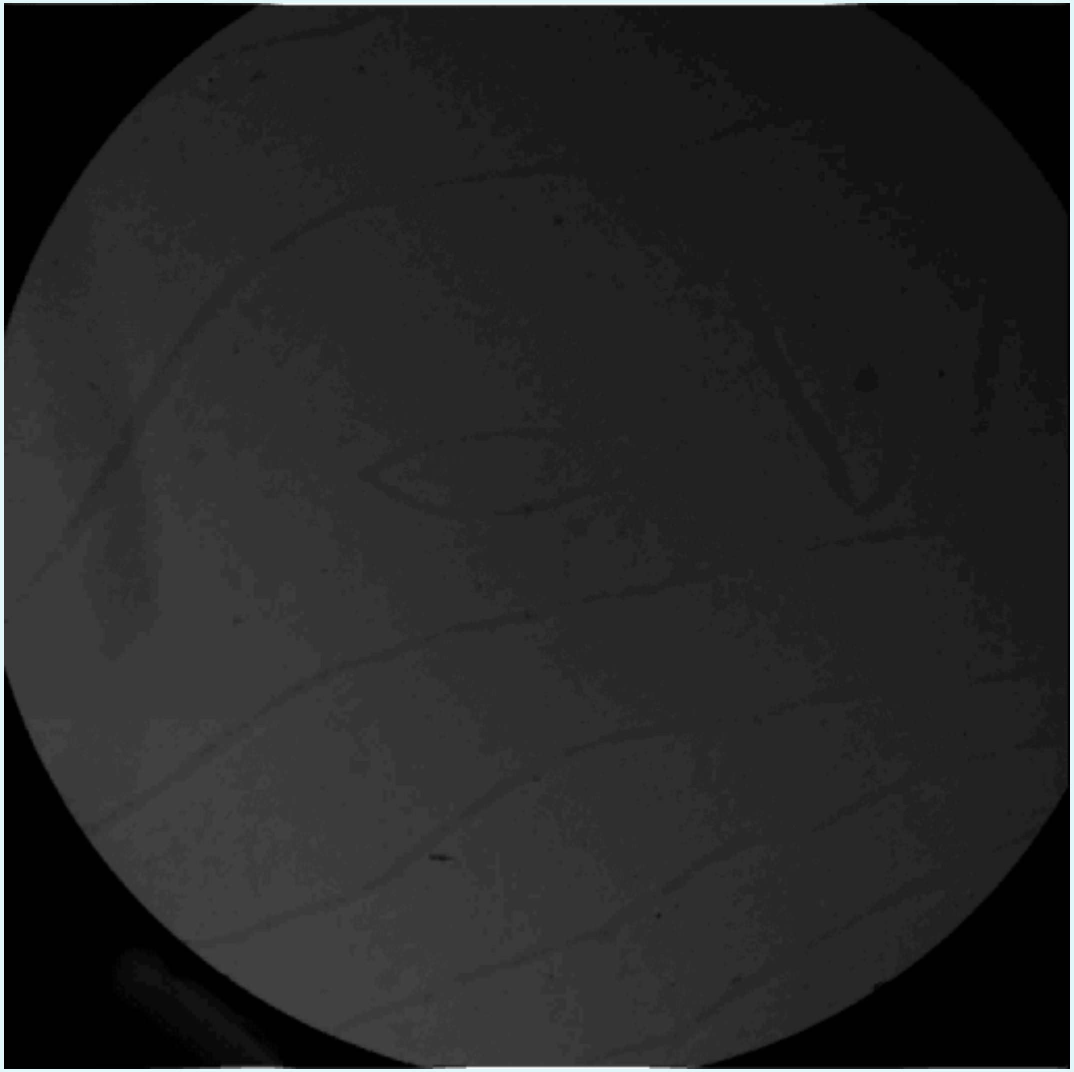

Th. Schmidt and E. Bauer, Phys. Rev. B 62 (2000) 15815

Interfactant effect

Pb on Si(111)

280 K

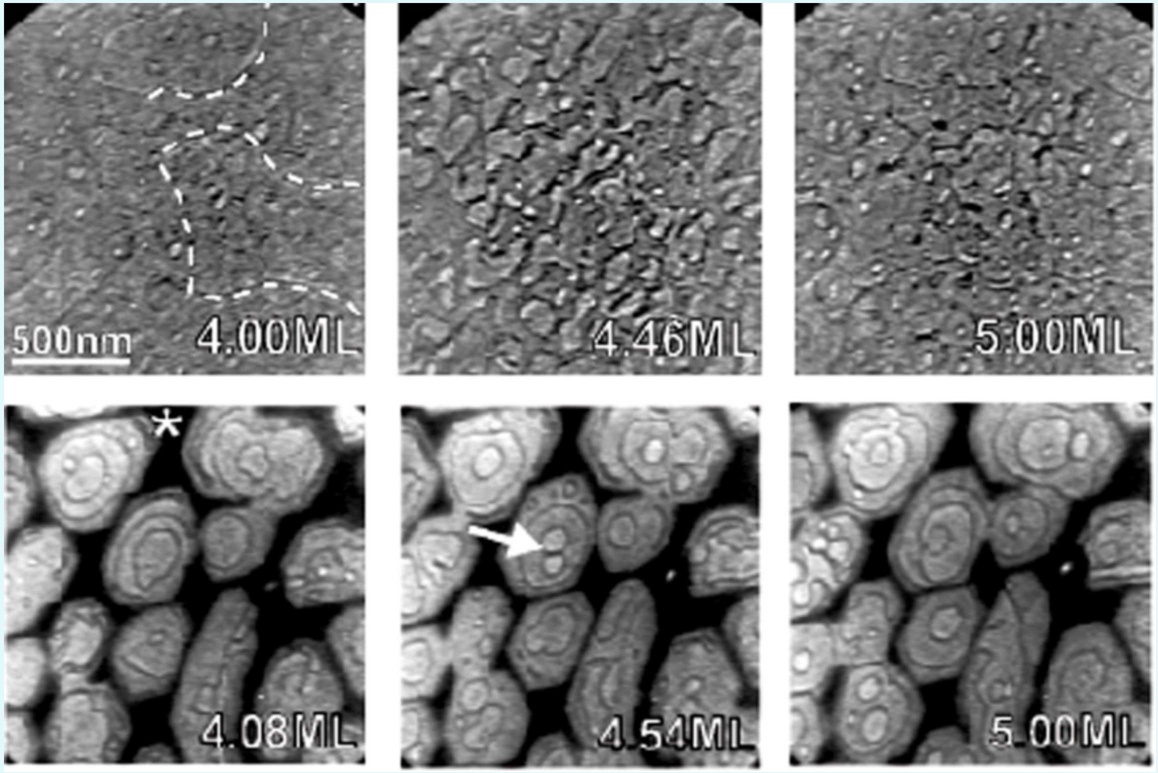

with

interfactant

without

Th. Schmidt and E. Bauer, Phys. Rev. B 62 (2000) 15815

Atomistic aspect: Nucleation rate

Maximum island density in the first Pb monolayer on various substrates

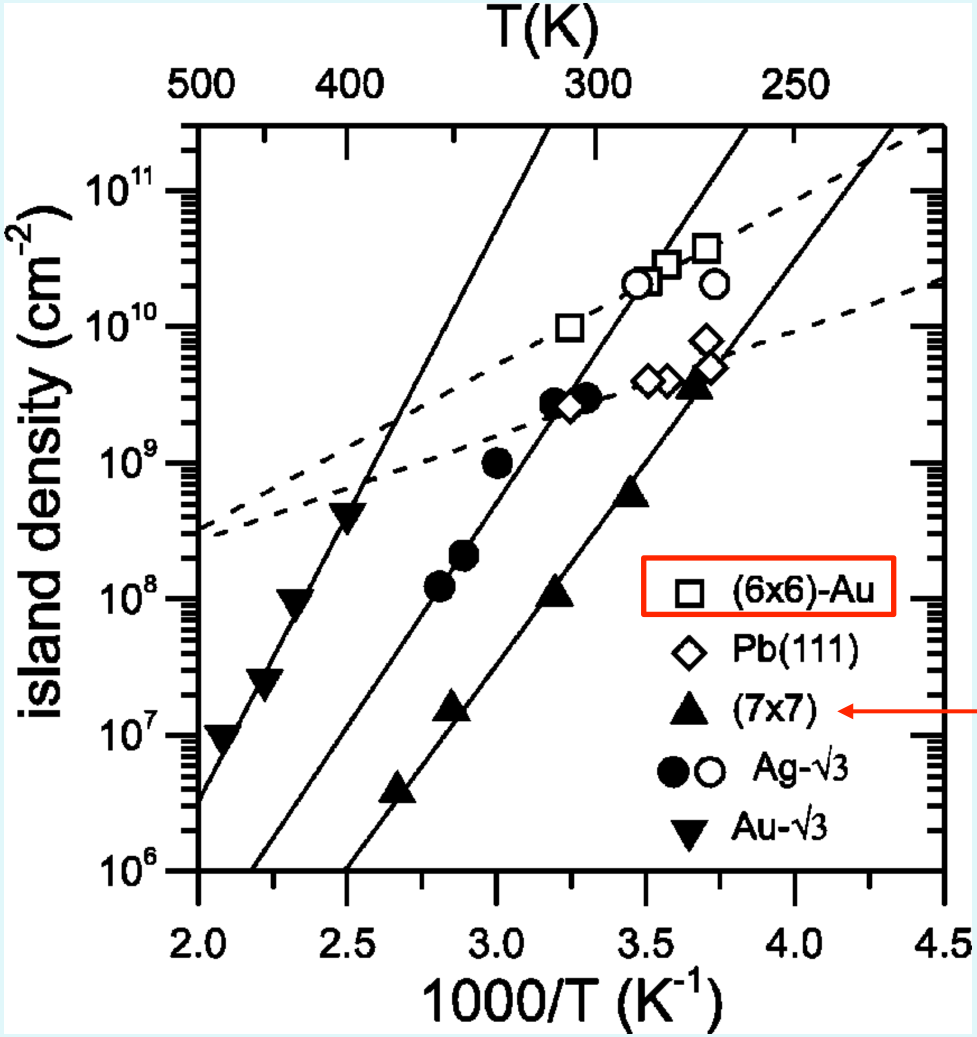

Clean Si(111)

Th. Schmidt and E. Bauer, Phys. Rev. B 62 (2000) 15815

Stranski-Krastanov growth

$\gamma_f < \gamma_s \quad \gamma_i > 0$ (strain!)

γ_i more important than $\gamma_f - \gamma_s$

γ_i determined by packing density difference between film and substrate

Example 1: densely-packed surfaces
(111) planes of fcc metals on W(110) surface

Metal	Density relative to W
Pb	0.668
Ag	0.980
Au	0.984
Pd	1.08
Cu	1.25
Ni	1.32
Co	1.37

Note: Number of stable 2D layers depends on temperature. Metastability!

Stranski-Krastanov growth

Pb on W(110) $\gamma_f << \gamma_s$ very large packing density difference

2D gas (dark) → 2D crystallization (bright) → 3D crystallization

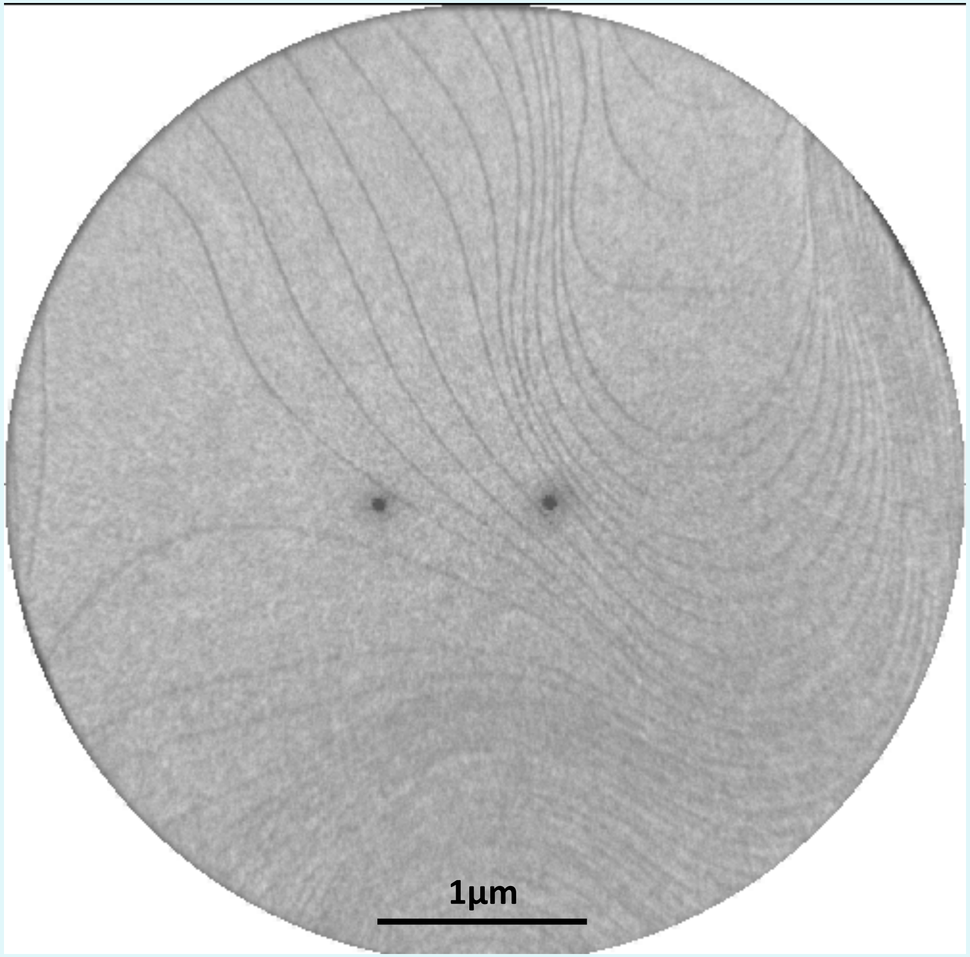

200 °C, 7.5 eV

T. Yasue et al, J. Phys.: Condens. Matter 21 (2009) 314024

Stranski-Krastanov growth

Au on W(110) $\gamma_f < \gamma_s$ small packing density difference

1 Ml → 2 ML → 3 ML → 4 ML unstable, break-up

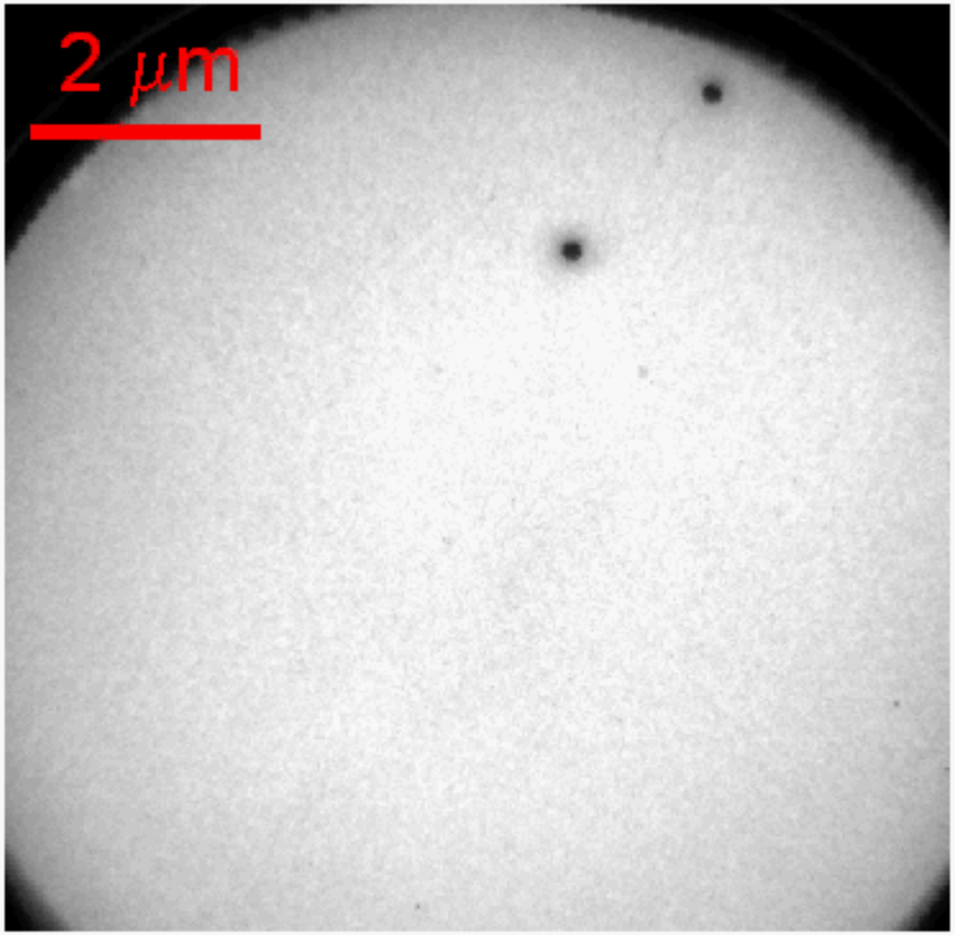

520 °C 7.6 eV 6 min/ML

T.O.Mentes et al, Elettra 2012

Stranski-Krastanov growth

Cu on W(110)

1 ML → 2 ML → compression → 3 ML +3D crystals (kinetic limitations)

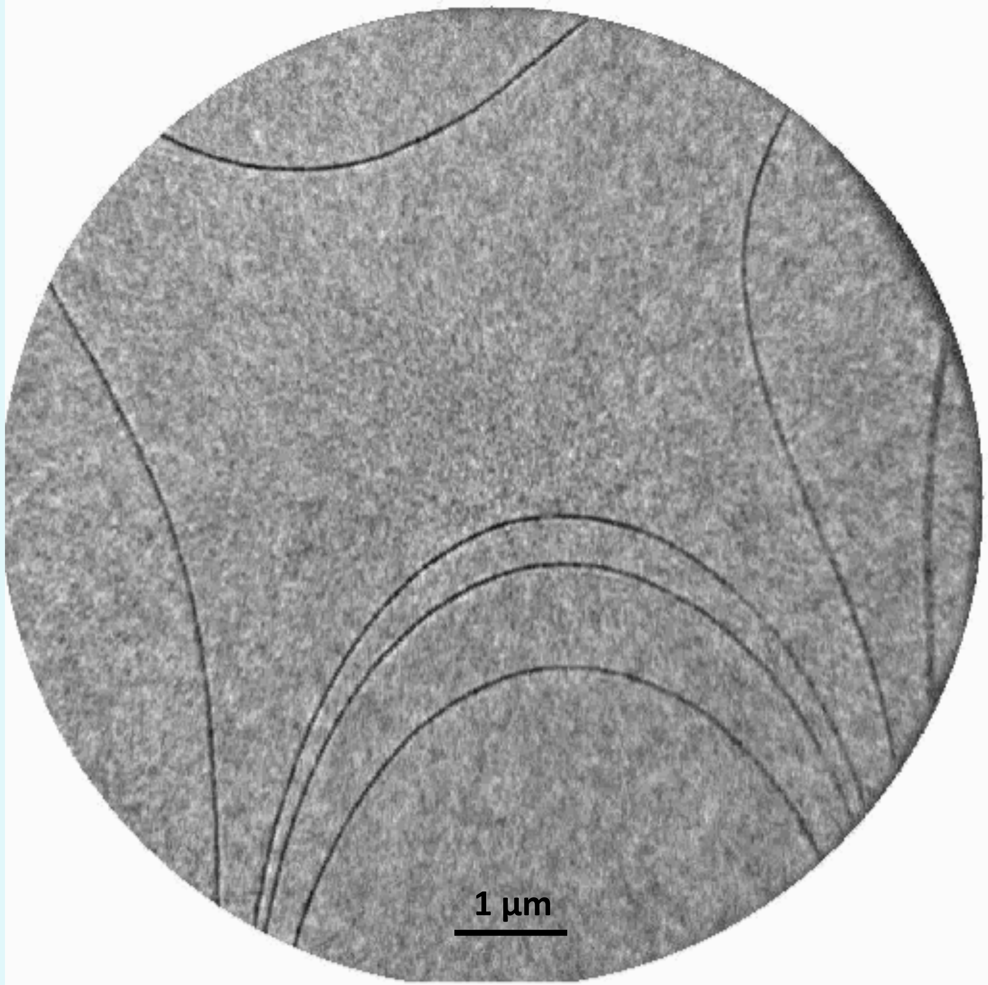

85 °C 7.5 eV

T. Koshikawa et al, ALC'05, 2006

Stranski-Krastanov growth

Cu on W(110)

1 ML → 2 ML → 3 and 4 ML quasi-simultaneous (electronic effect?)

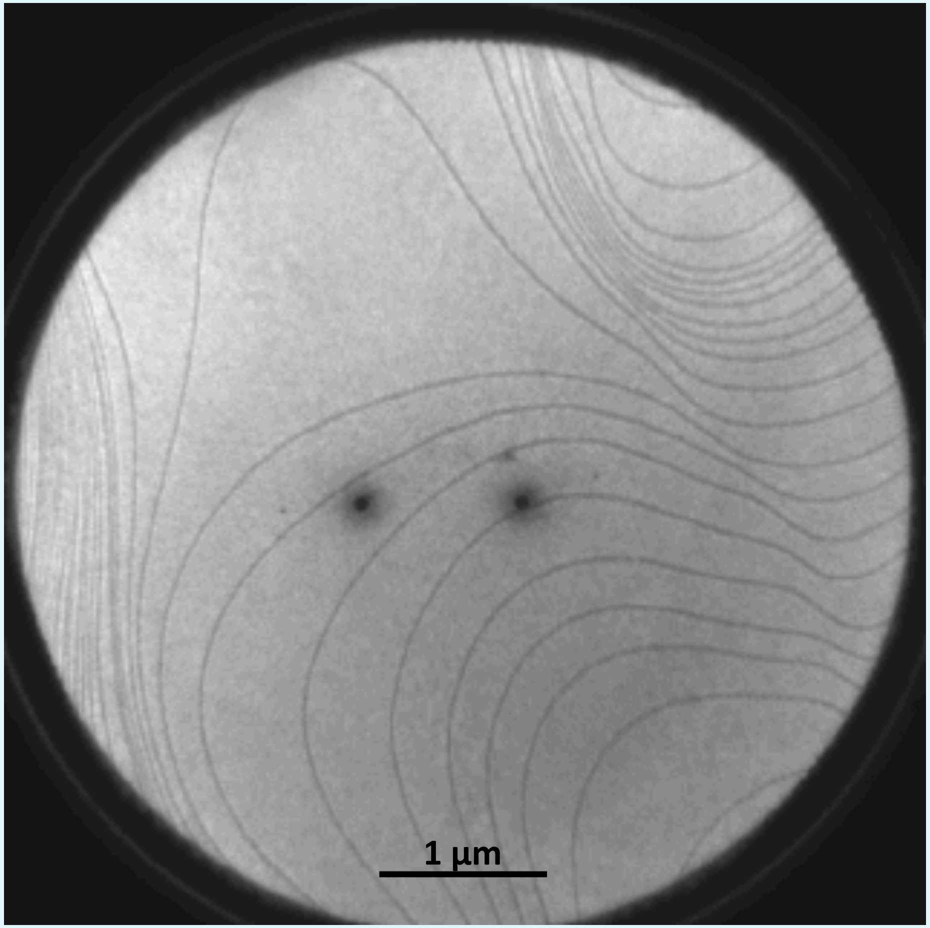

200 °C 7.5 eV

T. Koshikawa et al, ALC'05, 2006

Stranski-Krastanov growth

Co on W(110)   Very large misfit

1 ps ML → 1cp ML → 2 → 3 +1 → 3 + 4 ML, anisotropic stress effects, break-up

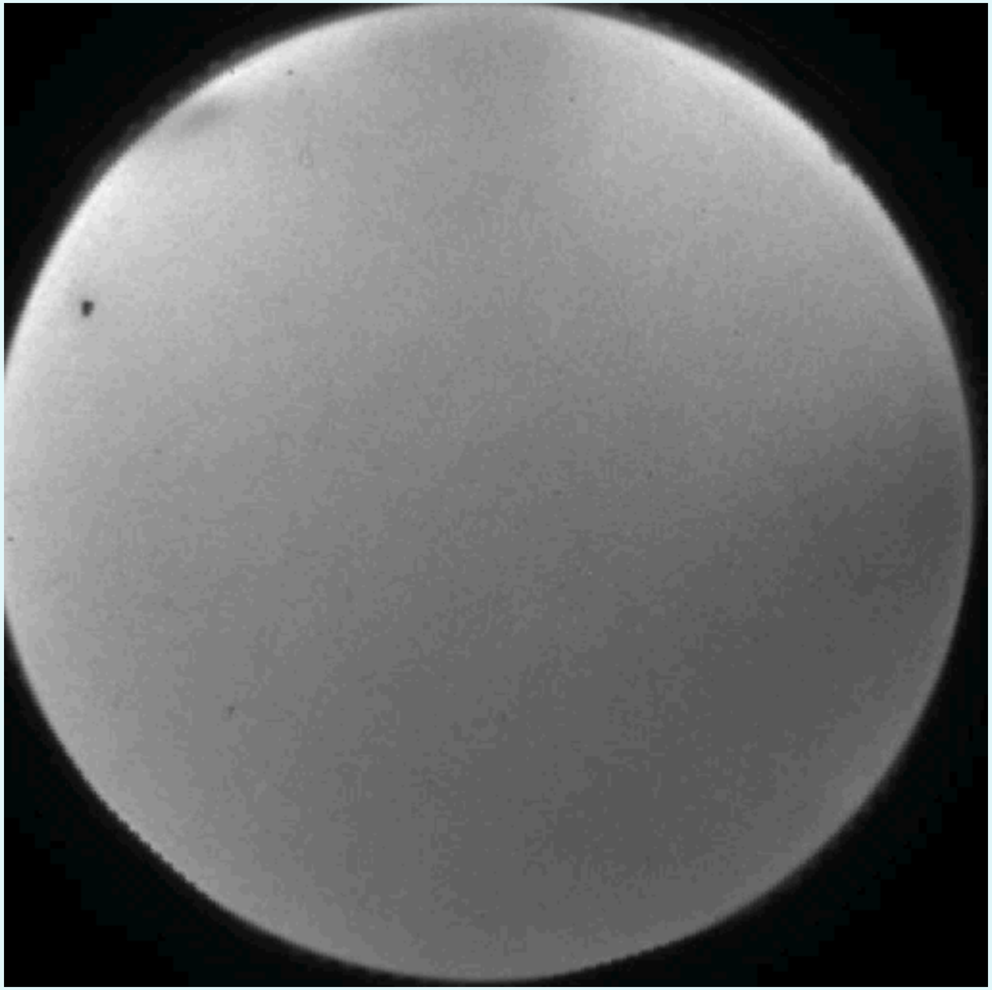

M. Suzuki et al, private communication 2015

Stranski-Krastanov growth

Growth of Co on W(110)

M. Suzuki OECU 2015

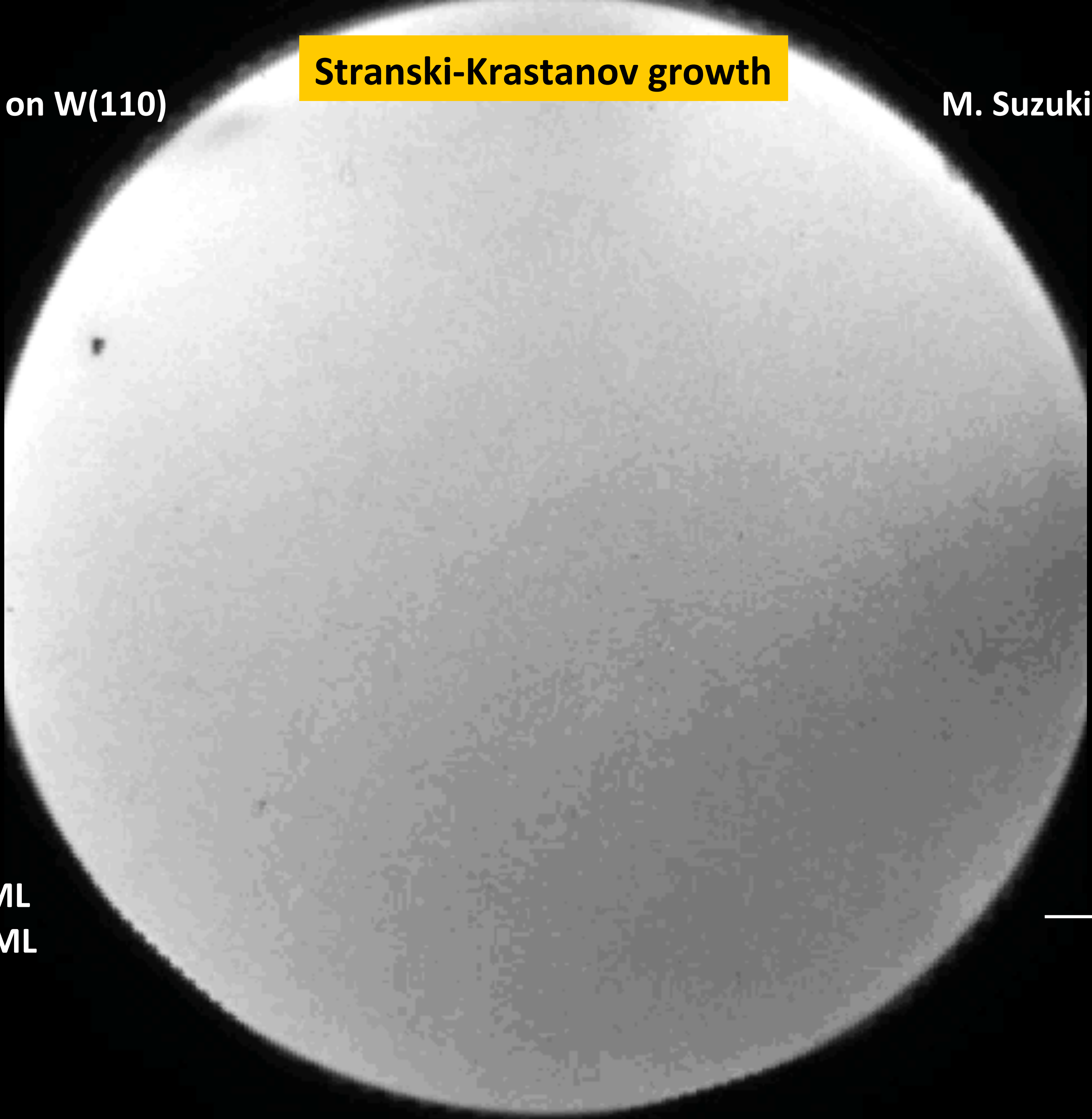

400 K
8.5 min/ML
Final 3.5 ML
2 eV

1 µm

Angle-resolved photoemission during growth of Co on W(110)

Strong influence of the pseudomorphic to close-packed transition on electronic structure

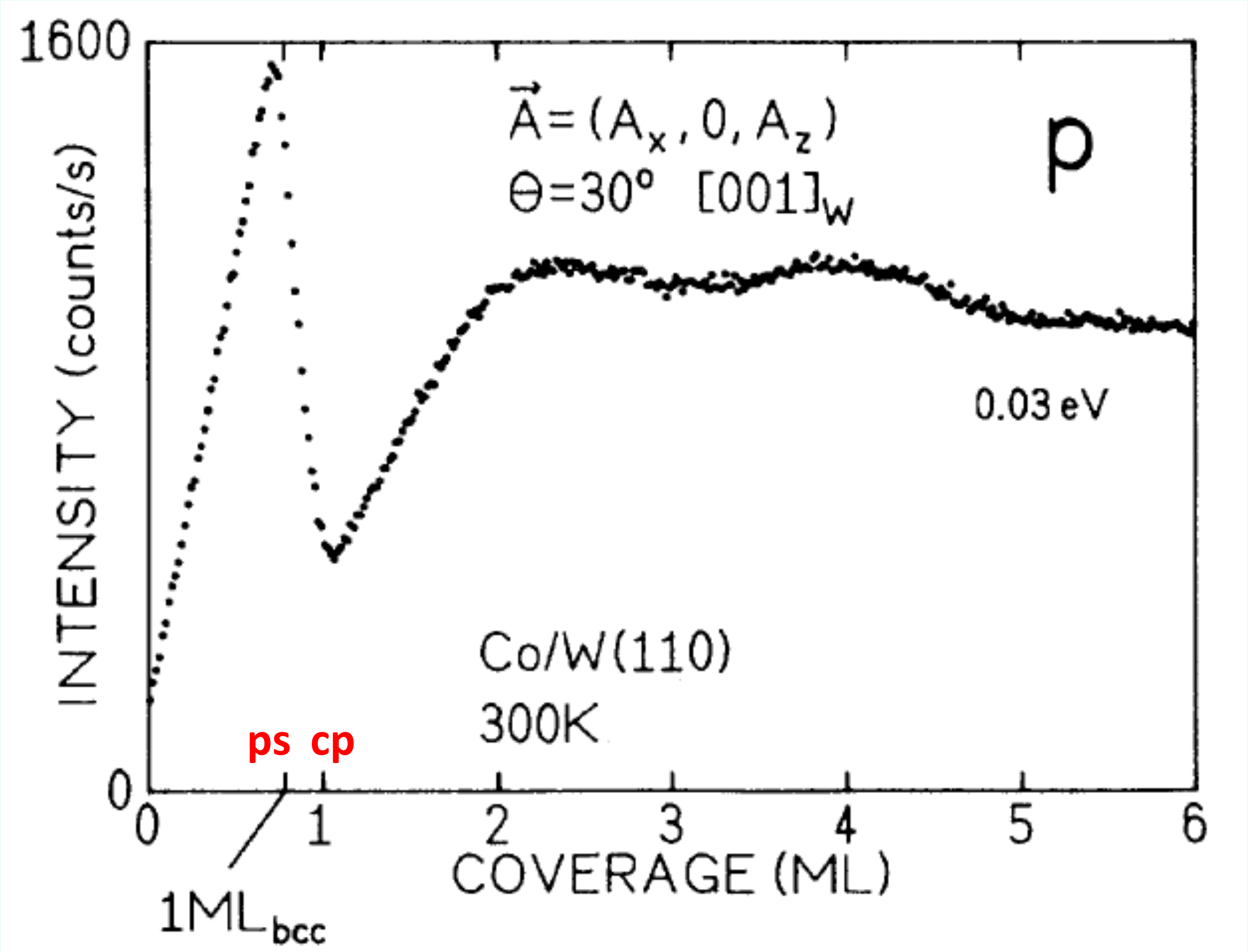

H. Knoppe and E. Bauer, Phys. Rev. B 48, 1794 (1993)

Stranski-Krastanov growth

Example 2: open surfaces
Metals on Mo, W(100) surfaces

Relative packing densities
Ag : Mo 0.97
Fe : W 1.22

Ag on Mo(100): Place exchange and 2D alloying below 1 ML

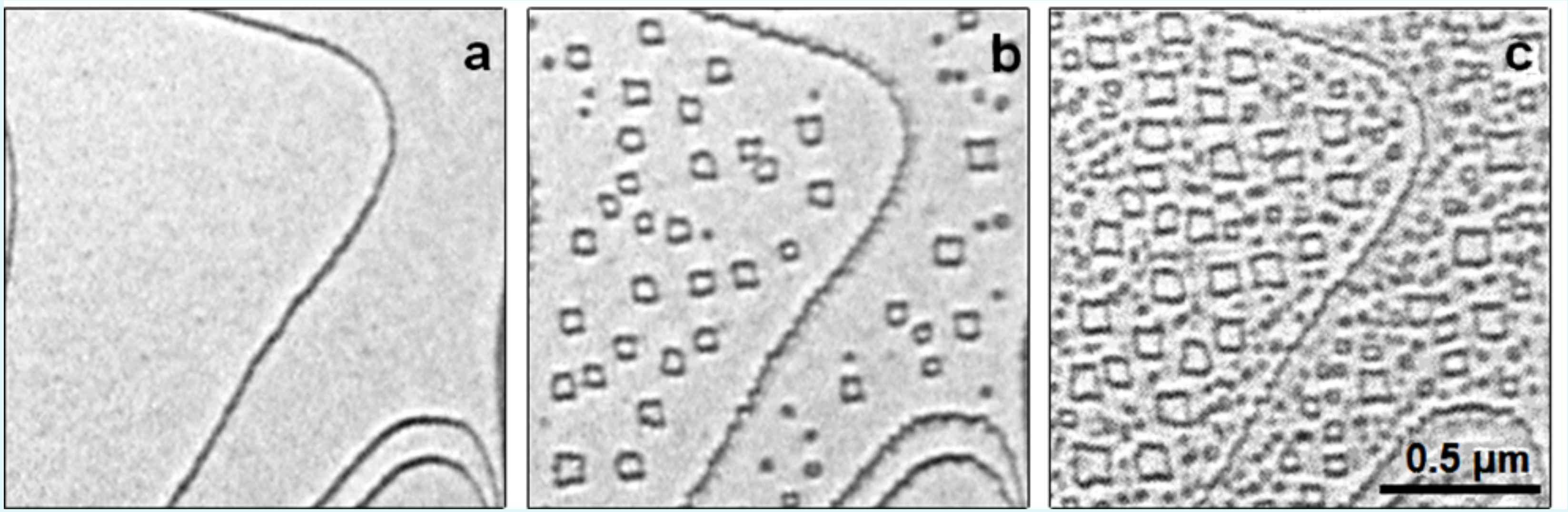

0 ML **0.16 ML** **0.38 ML**

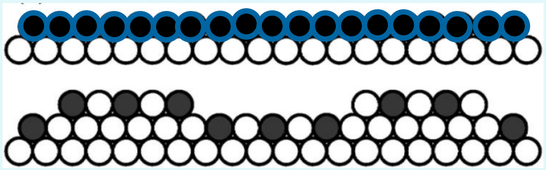

1 ML

0.5 ML

Very little strain

K. L. Man et al, Phys. Rev. B 74, 085420 2006

Stranski-Krastanov growth

3D growth on a thermodynamic stable pseudomorphic 2D double layer

Fe on W(100) at 800 K

Very high strain: lattice constant of Fe 10% larger than W

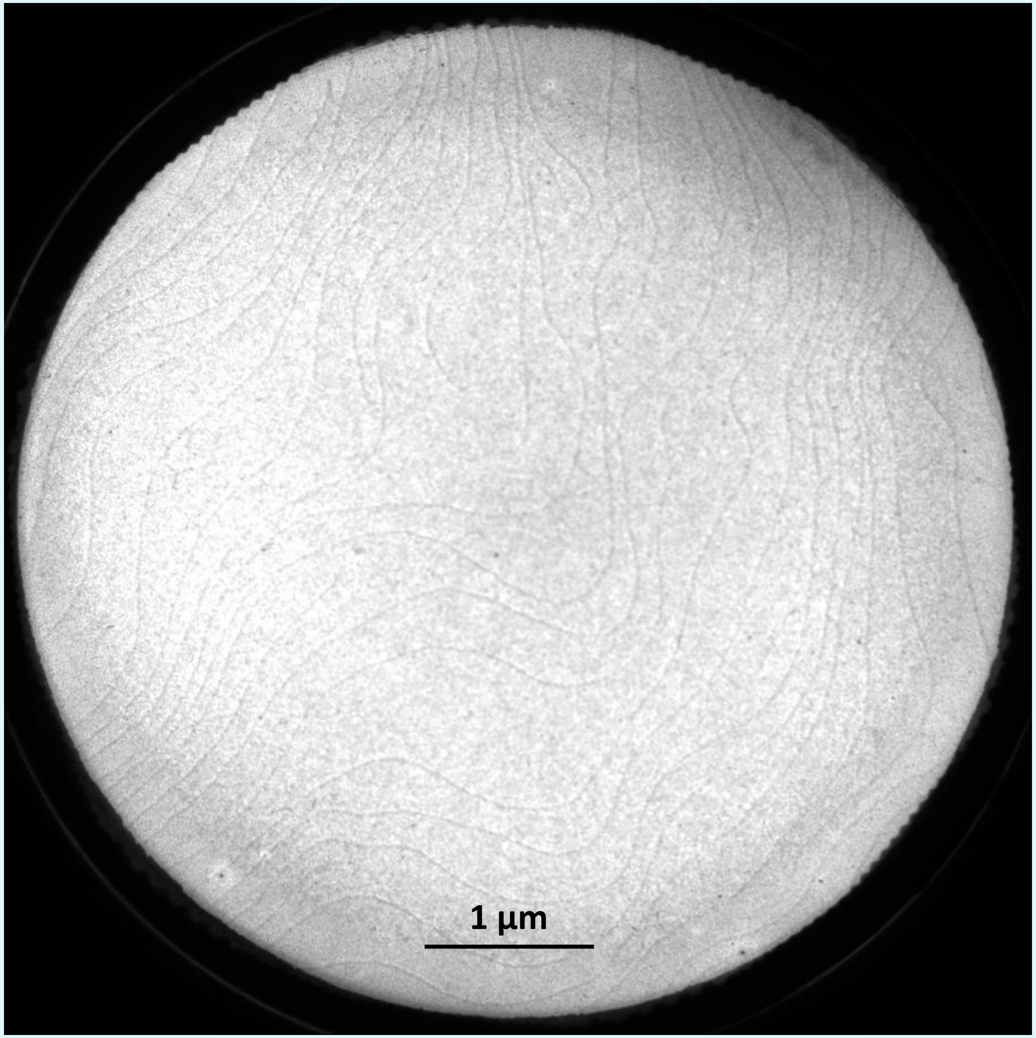

9 eV

{310} facets from LEED: (00) beam off axis: dark

Y. Niu et al, to be published

Stranski-Krastanov growth

2D → 3D transition from metastable pseudomorphic state

Fe on W(100) at 600 K

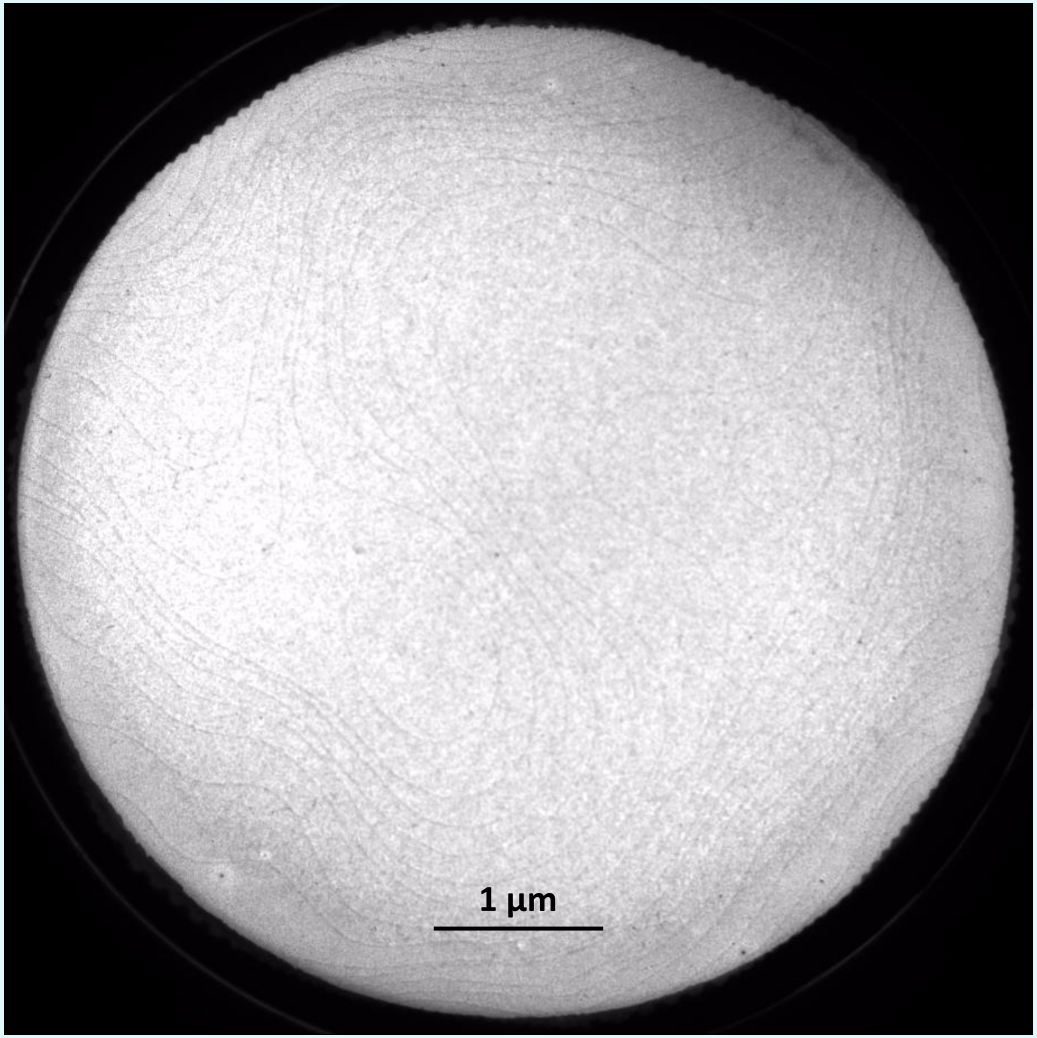

9 eV

3D nucleation at 3.2 ML
and 3D growth on 2 ML
consuming material
in excess of 2 ML

Y. Niu et al, to be published

Growth monitoring via LEEM intensity (00) beam

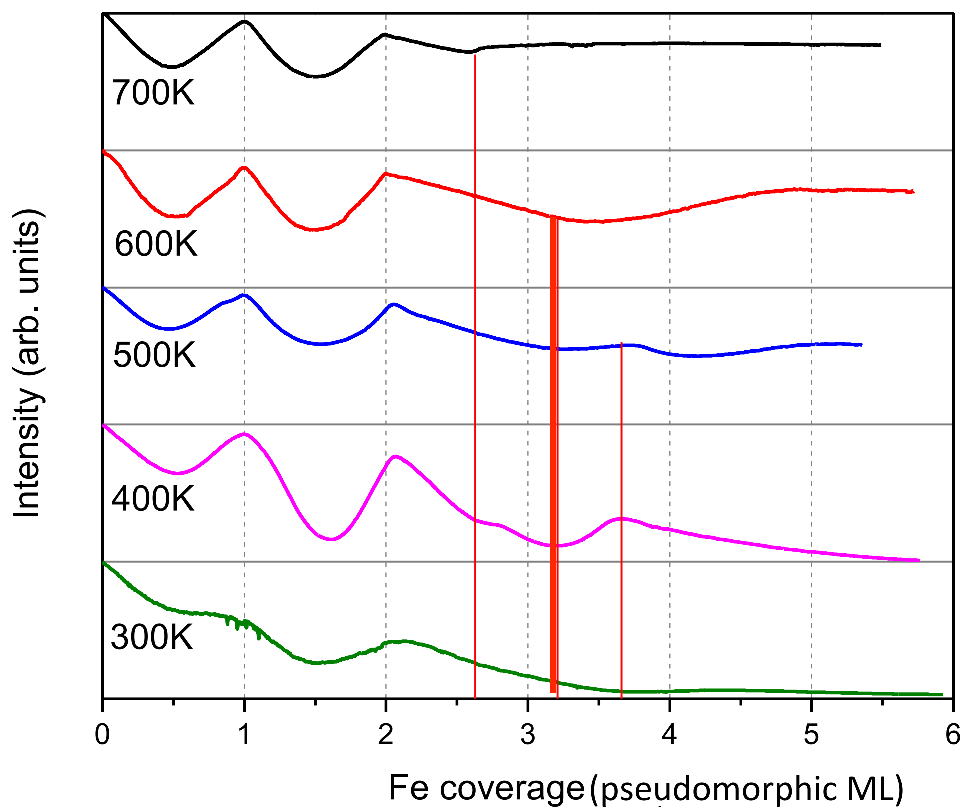

Red lines indicate 3D nucleation
9 eV

Y. Niu et al, to be published

Stranski-Krastanov growth

Transition 2D to 3D growth

In on Si(111)

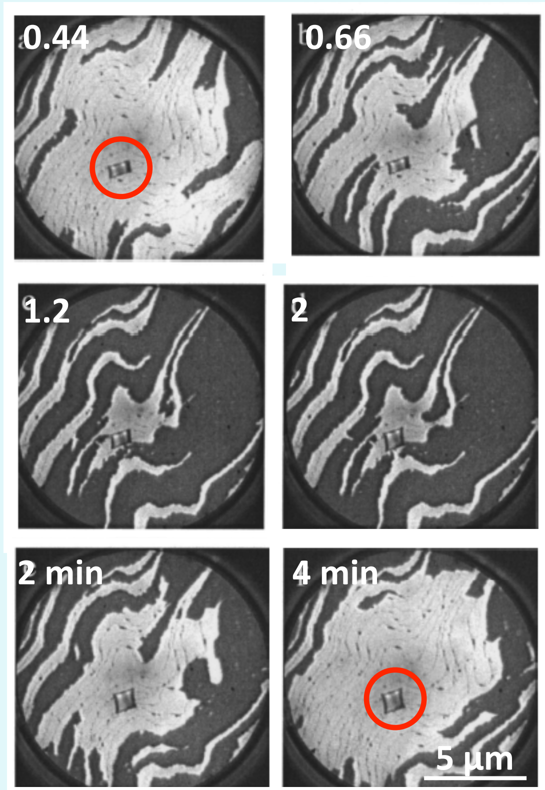

Top: Number of MLs beyond 2 ML
Bottom: time after deposition

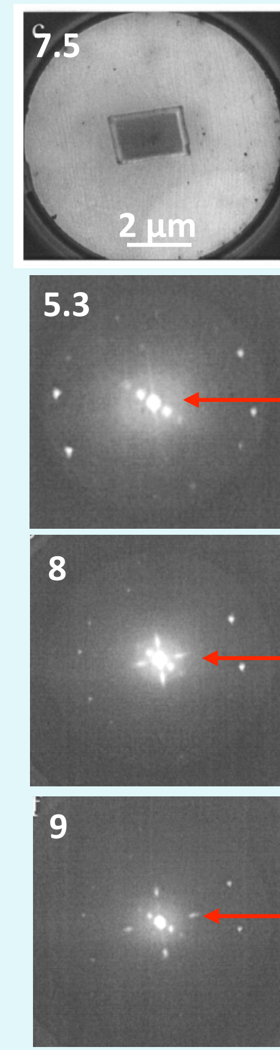

3D crystal
Information
from µLEED

Reconstruction
of top (100) surface

Side planes
{111} facets

Room temperature, 7.5 eV

A. Pavlovska et al, J. Vac. Sci. Technol. B 20, 2478 (2002)

Reactive Stranski-Krastanov growth

Cu on Si(111)

2D "5x5" silicide layer → 3D silicide crystals

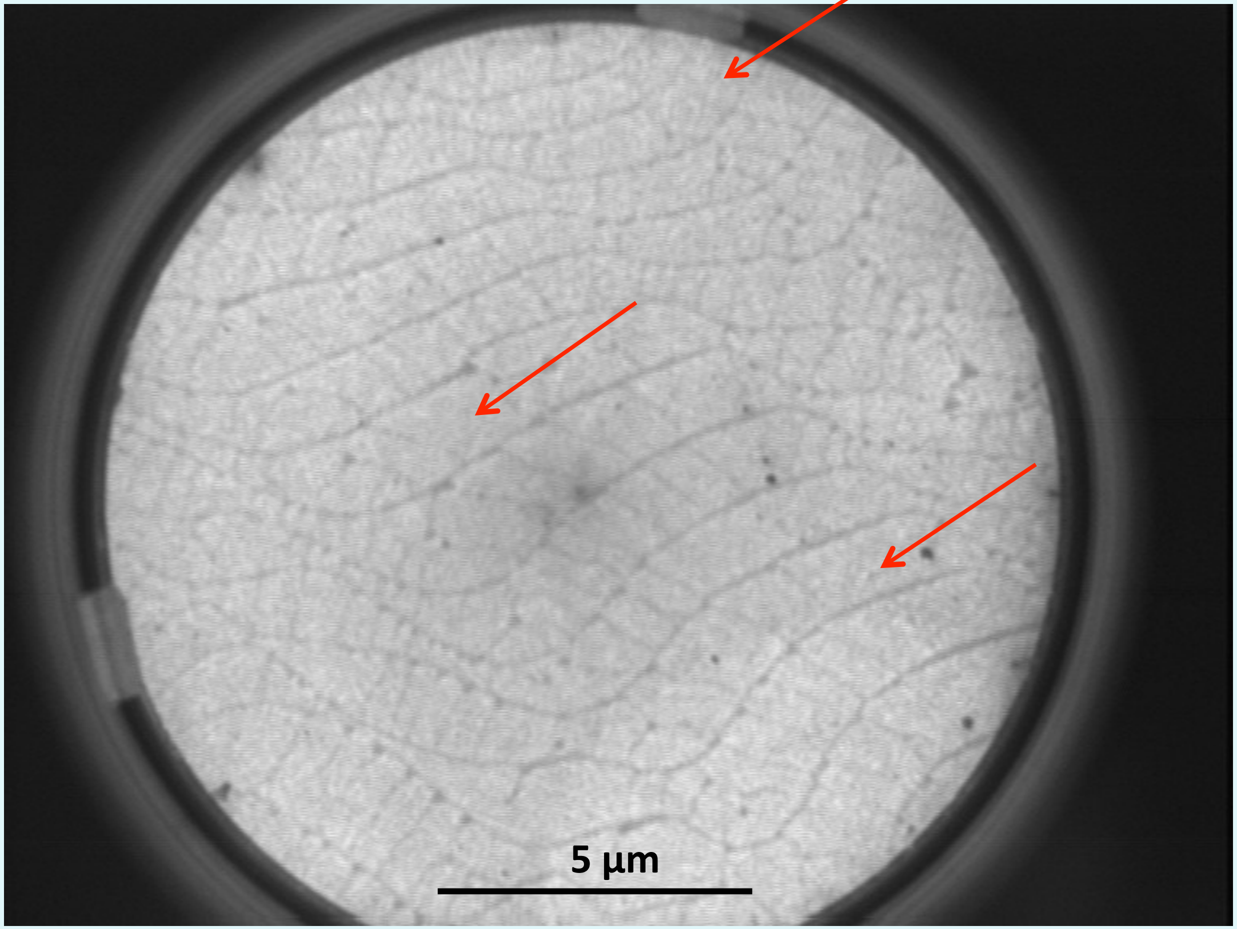

600 °C

T. Yasue et al, Surf. Sci. 480, 118 (2001)

Reactive Stranski-Krastanov growth

Cu on Si(111)
beyond the 2D reaction layer:
2D + 3D silicide

850 K

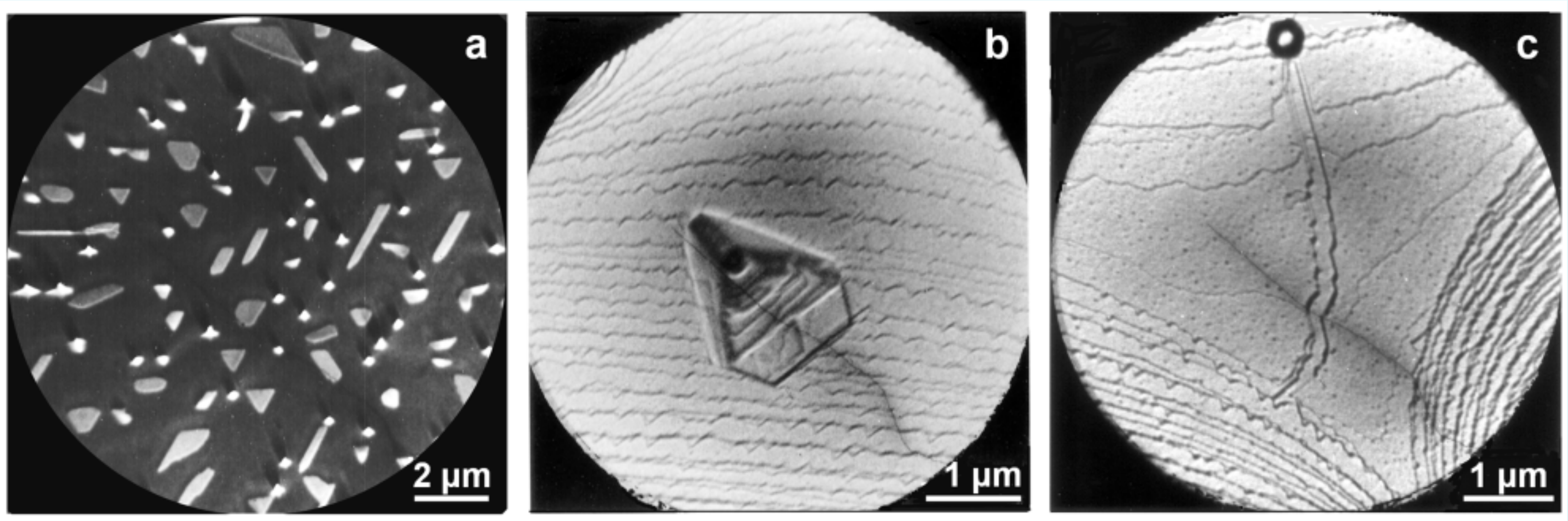

PEEM overview: Several epitaxial orientations

Reactive diffusion of small crystals

M. Mundschau et al, J. Appl. Phys. 65, 4747, 1989

Reactive Stranski-Krastanov growth

$Si_{1-x}Ge_x$ quantum dot growth on Si(100)

from Si_2H_6 + Ge_2H_6 at 650 °C – 700 °C

LEEM

SEM

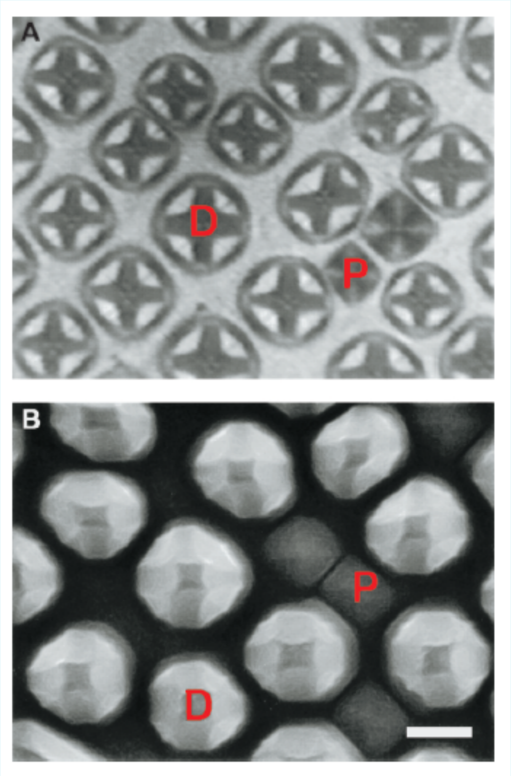

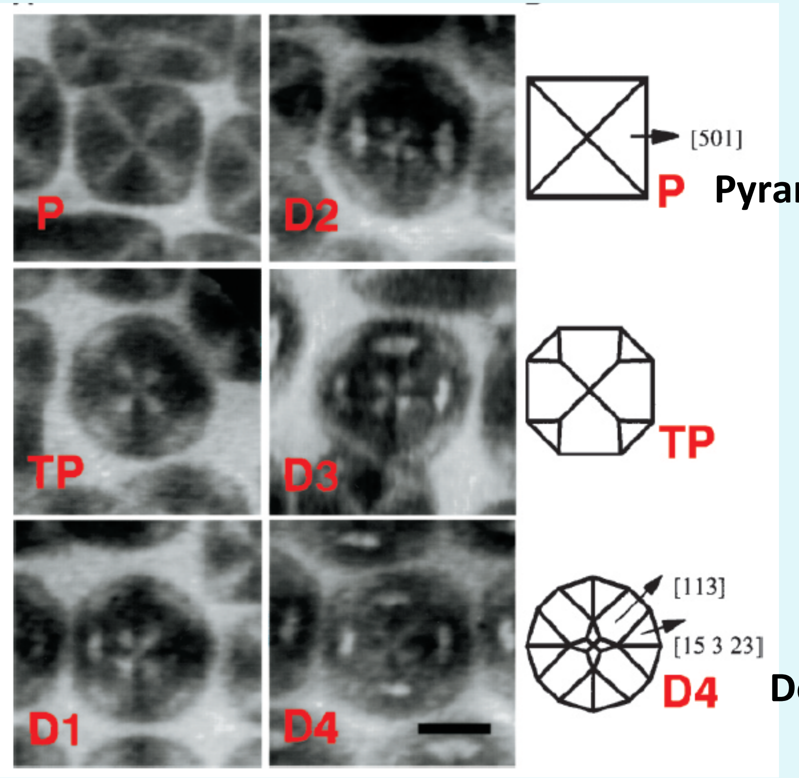

Growth without nucleation

R. M. Tromp et al, Phys. Rev Lett. 84, 4641 (2000)

F.M. Ross et al, Science 286, 1931 (1999)
R. M. Tromp, F. M. Ross, Annu. Rev. Mater. Sci. 30, 431 (2000)

Reactive Stranski-Krastanov growth

γ: $Si_3N_4 > Si$

Si nitride growth on Si(111) exposed to NH_3

Clean, 1180 K, 2×10^{-7}

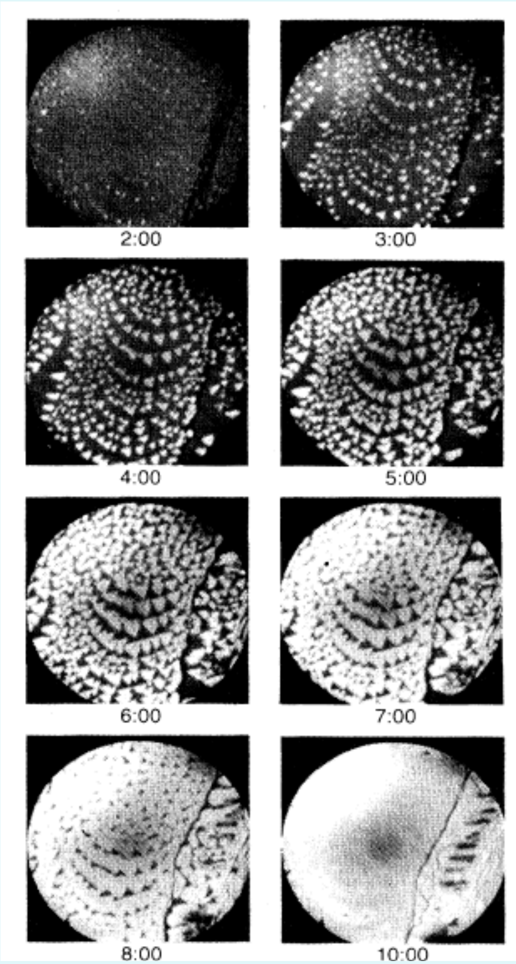

Light contamination
1270 K, 1×10^{-7}

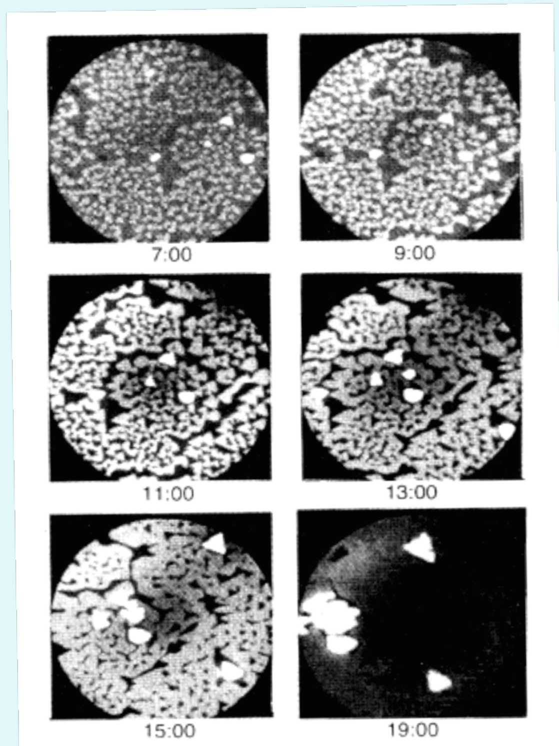

Strong contamination
1200 K, 1.5×10^{-7}

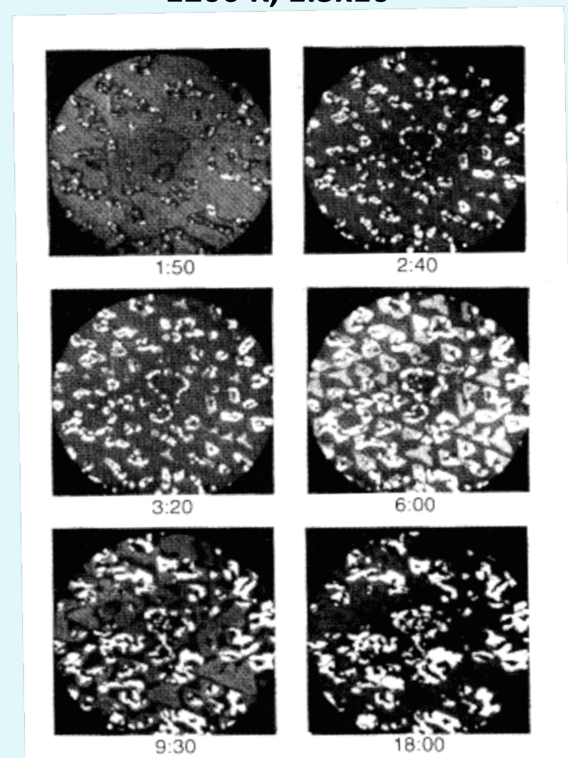

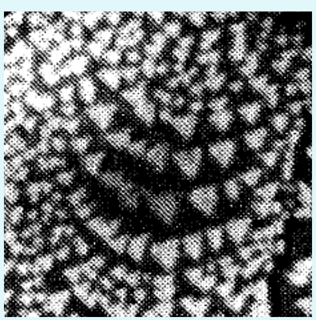

Video frames, E =42 eV, field of view 10 µm (left), 15 µm (center, right)

Suppression of 2D growth by contamination

Still good Si(111)-(7x7) on right side

E. Bauer et al, Phys. Rev. B 51, 17891 (1995)

Reactive Volmer-Weber growth

$\gamma_f > \gamma_s$

$CoSi_2$ on Si(111): very small misfit 1.2 %

Formed by Fe deposition

Growth at about 800 °C

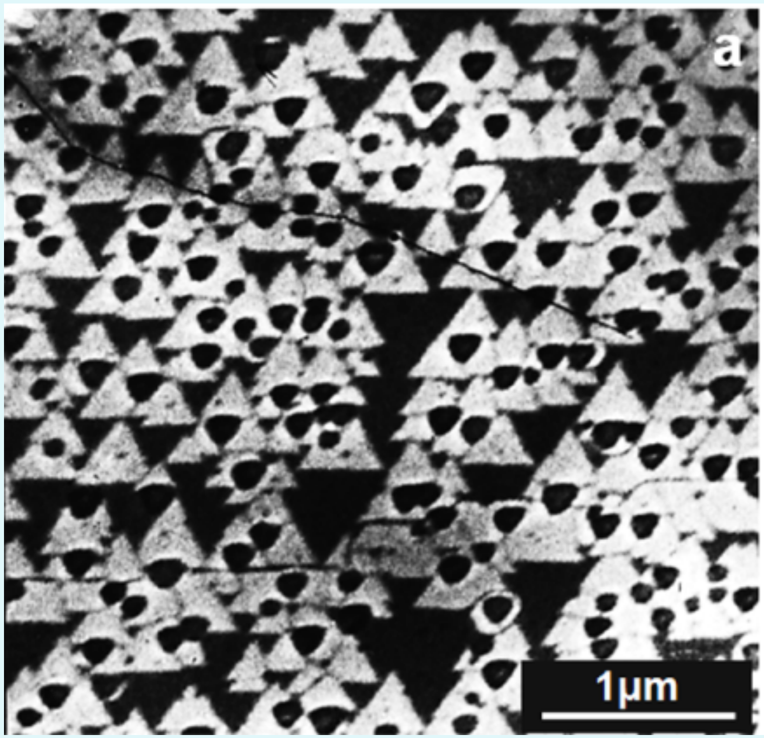

After long sublimation at about 1100 °C

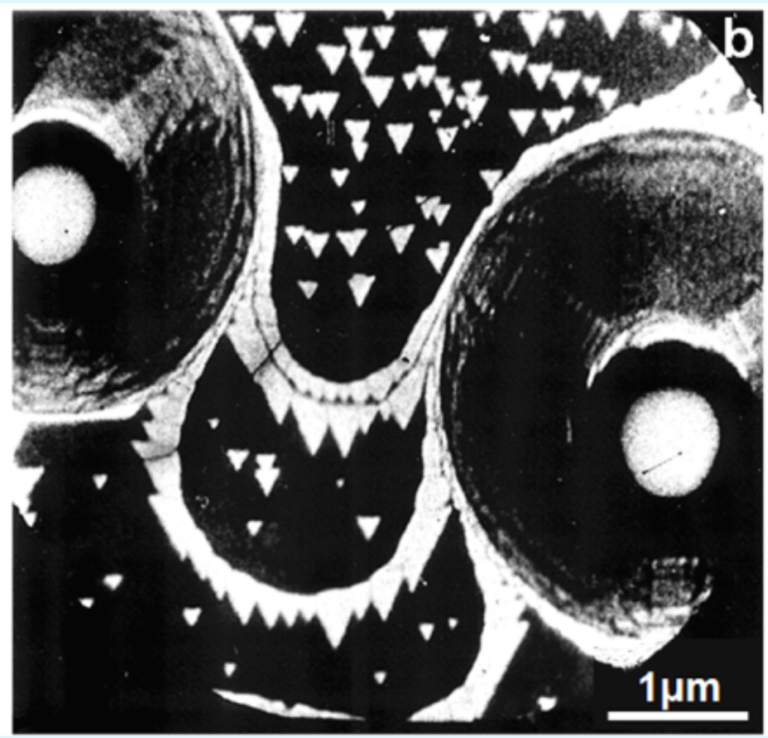

10 eV

Small inverted triangles $CoSi_2$
Large bright triangles Si(111)-(7x7)
Large dark triangles Si(1x1)

Si sublimation hillocks capped by $CoSi_2$

E. Bauer et al, J. Vac. Sci. Technol. A 9, 1007 (1991)

Spectroscopic Photo Emission and Low Energy Electron Microscope

SPELEEM schematic

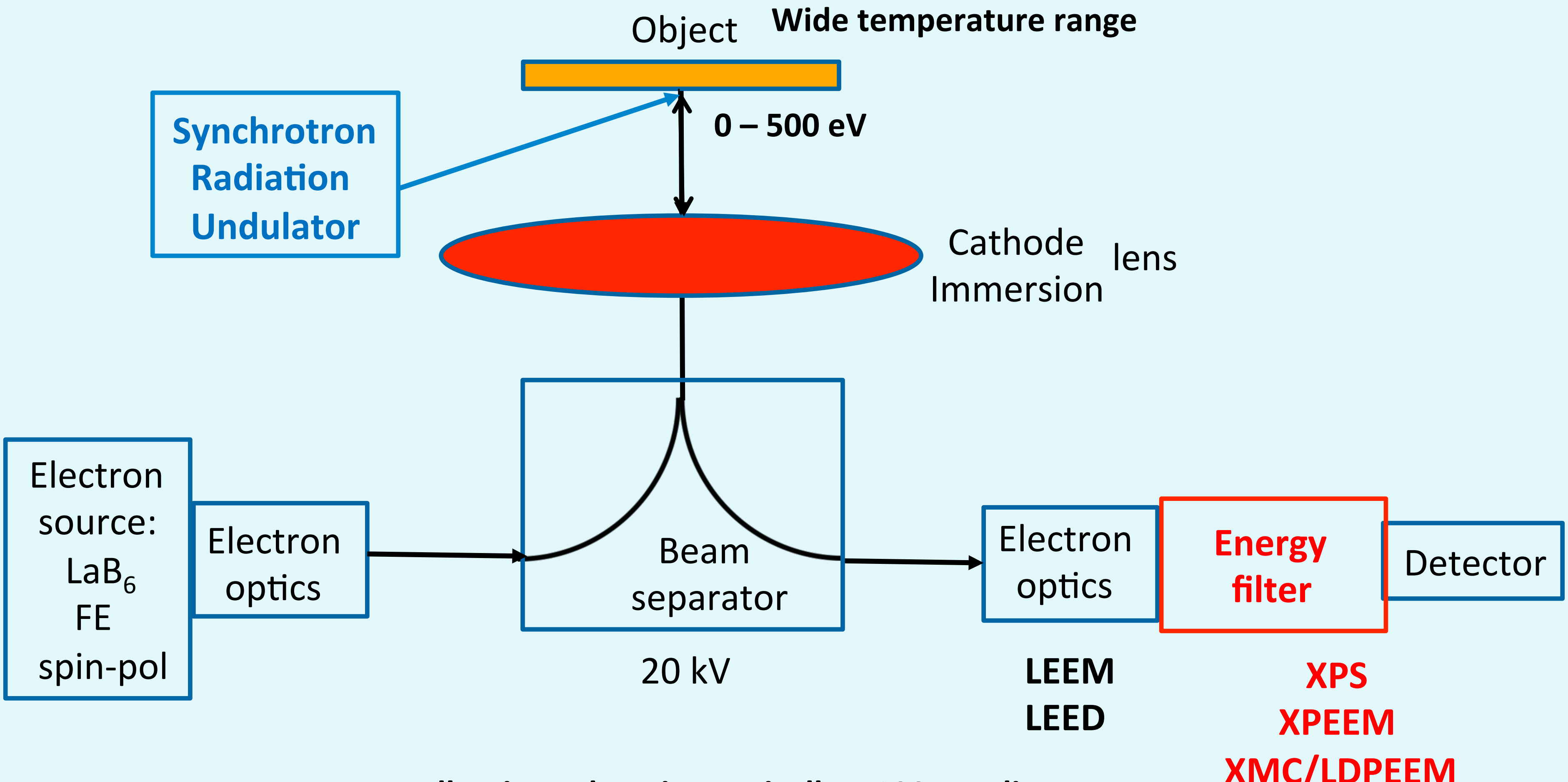

Illuminated region typically ≤ 100 µm diameter

In-situ evaporation and gas exposure at grazing angle of incidence 16° - 45°

Pressure ≤ 10^{-5} mbar

Multimethod epitaxy study with the SPELEEM

Fe on ZnS

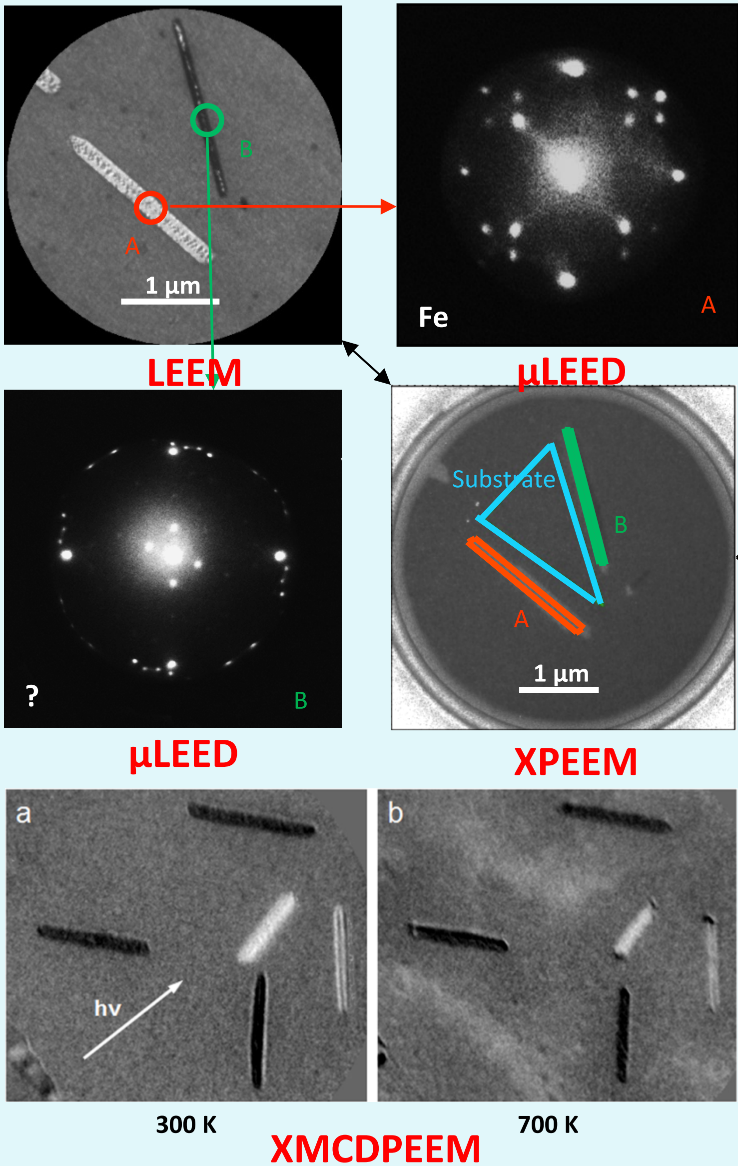

hν = 260 eV

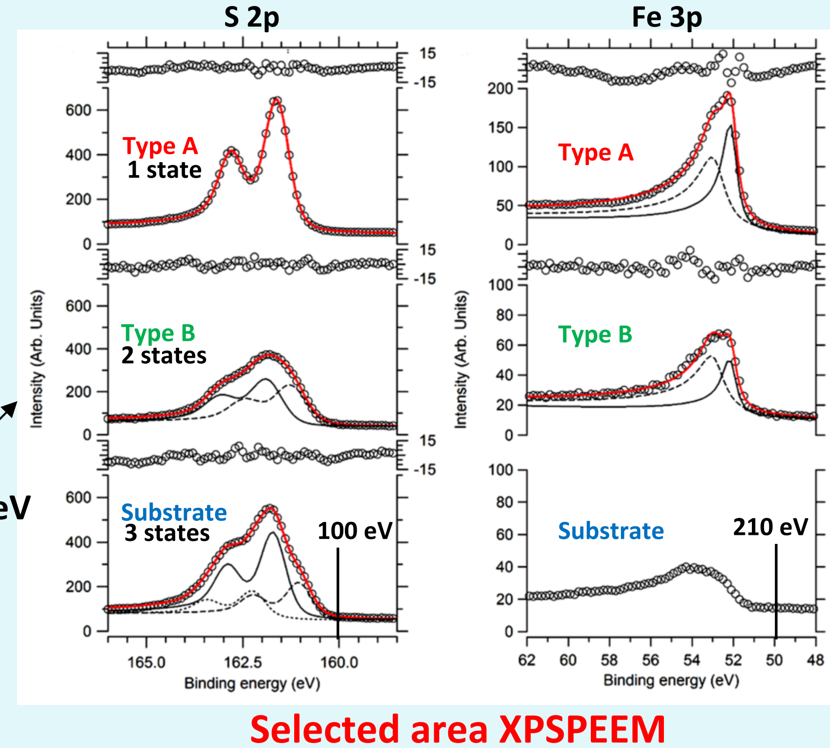

hν = 700 -725 eV

Crystal A:
Fe
Crystal B:
Greigite
Fe_3S_4

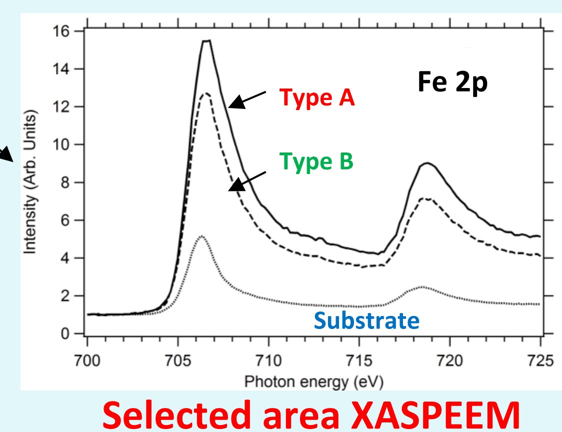

Bauer et al, J. Mater. Chem. A 2, 1903 (2014)

Greigite has many different epitaxial orientations anda shapes due to stacking defects

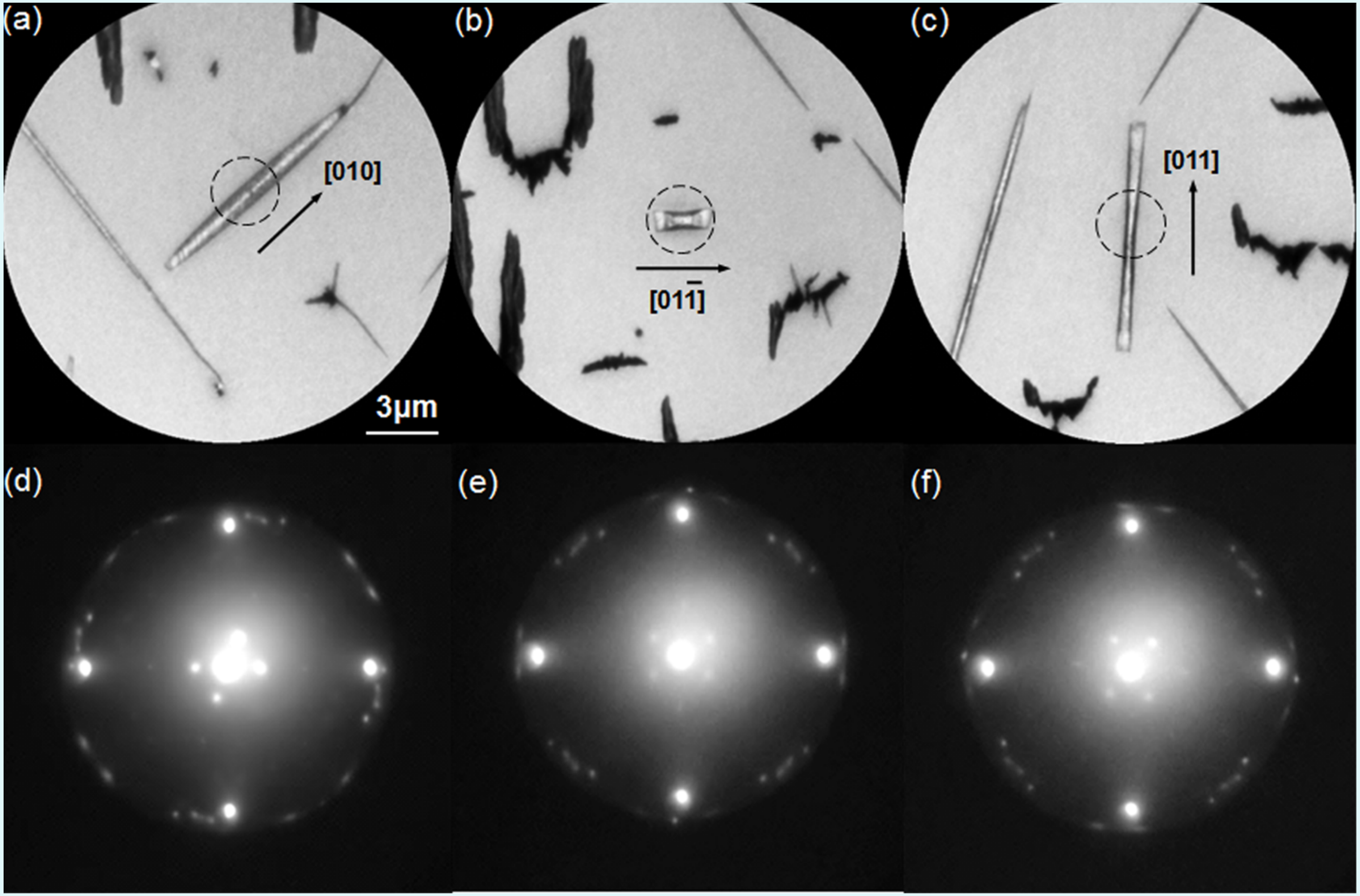

Fe on ZnS at 550 K

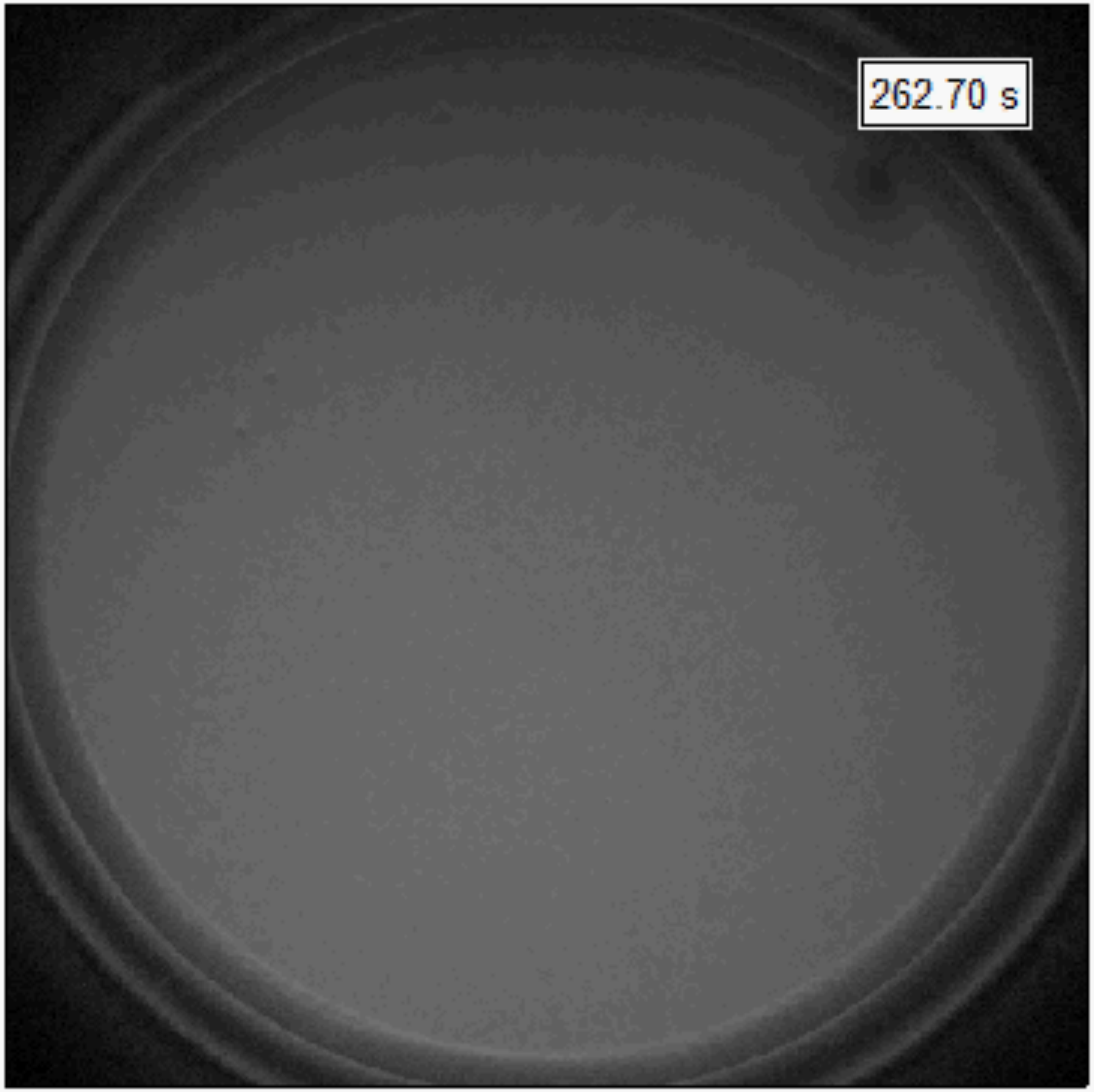

Man et al, unpublished 2013

The importance of stress anisotropy

Example: Au on W(110)

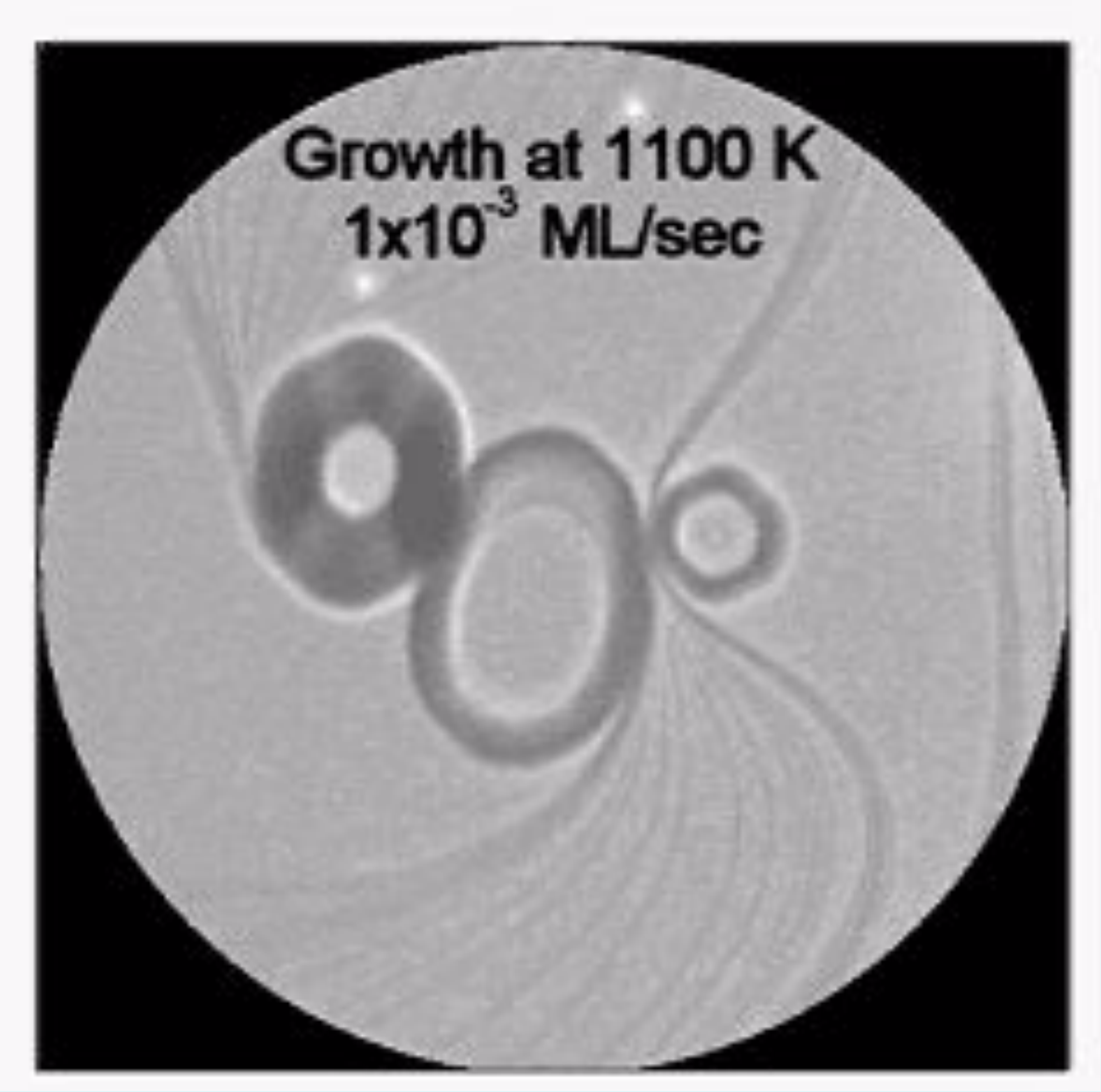

Duden 1996, Mentes, Locatelli, Bauer 2004

Stress anisotropy examples

Cu/Mo(110)

Au/W(110) Temperature dependence of stress anisotropy

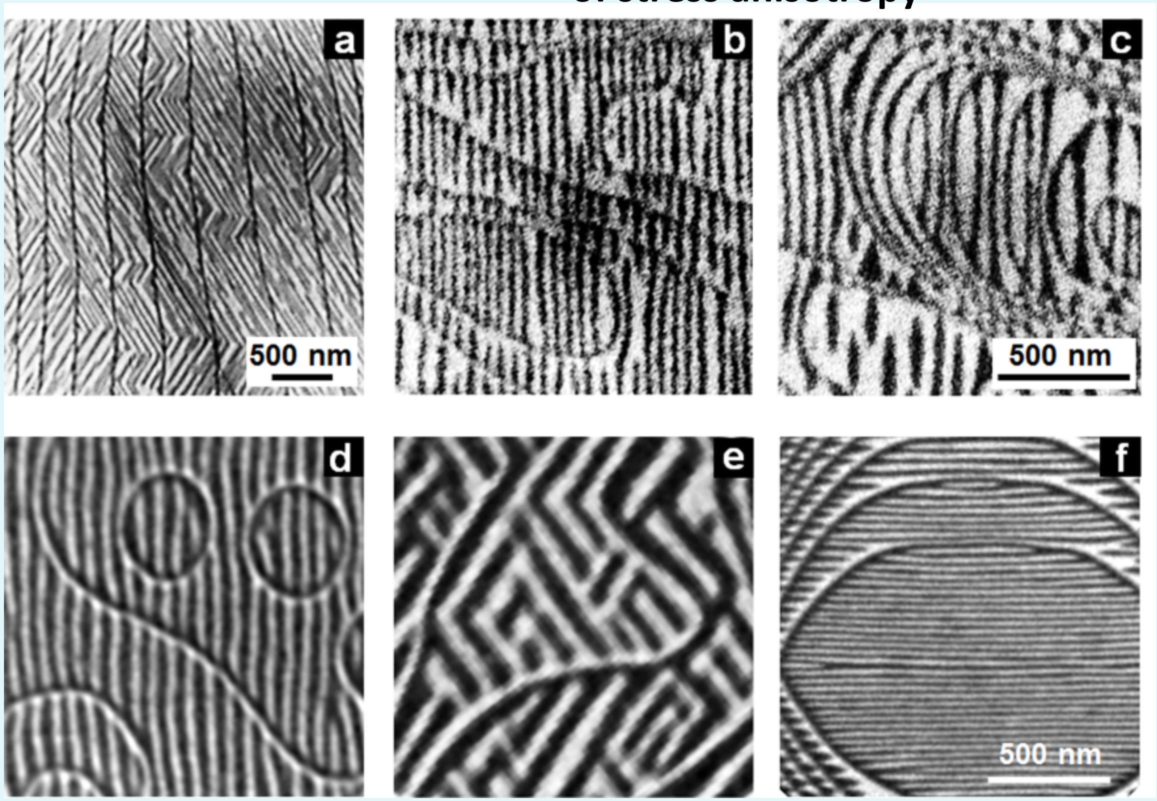

0 ML O   0.2 ML O   0.3 ML O

Pd/W(110): Stress anisotropy control by co-adsorption

a) M. Mundschau et al, 1989, unpublished

b, c) T. Duden, Ph.D. thesis 1996

d-f) T.O.Mentes et al, EPL 94, 38003 (2011)

Summary

Epitaxy has many faces.

At low supersaturation the growth is dominated by the interplay of surface and interface energies (growth modes!), with the strain energy included in the interface energy playing a dominating role. This is particularly evident in the sub-monolayer range.
With increasing supersaturation kinetic effects play an important role and lead to metastable configurations. Relaxations from these configurations with increasing thickness play an important role in epitaxy.

LEEM is an ideal tool for the study of epitaxial growth processes due to fast image acquisition, which allows real time studies and high structural sensitivity. Combined with LEED and synchrotron radiation-based imaging and spectroscopy it allows comprehensive characterization of epitaxial growth.

For more information see next slide, which shows many more results.

Ernst Bauer

Surface Microscopy with Low Energy Electrons

This book, written by a pioneer in surface physics and thin film research and the inventor of Low Energy Electron Microscopy (LEEM), Spin-Polarized Low Energy Electron Microscopy (SPLEEM) and Spectroscopic Photo Emission and Low Energy Electron Microscopy (SPELEEM), covers these and other techniques for the imaging of surfaces with low energy (slow) electrons. These techniques include Photoemission Electron Microscopy (PEEM), X-ray Photoemission Electron Microscopy (XPEEM), and their combination with microdiffraction and microspectroscopy, all of which use cathode lenses and slow electrons. Of particular interest are the fundamentals and applications of LEEM, PEEM, and XPEEM because of their widespread use. Numerous illustrations will illuminate the fundamental aspects of the electron optics, the experimental setup, and particularly the application results with these instruments. Surface Microscopy with Low Energy Electrons will give the reader a unified picture of the imaging, diffraction, and spectroscopy methods that are possible using low energy electron microscopes.

- Provides a unified description of full-field, low energy electron microscopies
- Presents the basic theory and experiment of low energy emission and reflection
- Compares the possibilities and limitations of the various imaging methods
- Describes multi-method studies
- Contains an extensive list of references for easy access to the original literature

Materials Science / Chemistry

ISBN 978-1-[illegible]

▶ springer.com

2014

Bauer

Surface Microscopy with Low Energy Electrons

Ernst Bauer

Surface Microscopy with Low Energy Electrons

Springer